8-1-2010

Agolohymena aspidocauda nov. gen., nov. spec., a Histophagous Freshwater Tetrahymenid Ciliate in the Family Deltopylidae (Ciliophora, Hymenostomatia), from Idaho (Northwest U.S.A.): Morphology, Ontogenesis and Molecular Phylogeny

William A. Bourland
Boise State University

Michaela C. Strüder-Kypke
University of Guelph

Agolohymena aspidocauda nov. gen., nov. spec., a Histophagous Freshwater Tetrahymenid Ciliate in the Family Deltopylidae (Ciliophora, Hymenostomatia), from Idaho (Northwest U.S.A.): Morphology, Ontogenesis and Molecular Phylogeny

William A. Bourland
Boise State University

Michaela C. Strüder-Kypke
University of Guelph

Abstract

Morphology, ontogeny and the molecular phylogeny of *Agolohymena aspidocauda* nov. gen., nov. spec., a new freshwater tetrahymenid ciliate from Idaho, U.S.A, are described. The ontogeny and histophagous mode of nutrition are similar to those of *Deltopylum rhabdoides* Fauré-Fremiet and Mugard, 1946. The new genus is placed with *Deltopylum* in the resurrected family Deltopylidae Song & Wilbert, 1989. We emend the diagnostic features of the family to include division by polytomy, right and left somatic kineties extending into the preoral suture, crook-shaped or sigmoid adoral membranelles 1 and 2, markedly reduced adoral membranelle 3 and a tetrahymenid silverline pattern. The main diagnostic features of the new genus are a disc-shaped caudal ciliary array and formation of two types of resting cysts, one smooth and the other bearing tangled tubular or cylindrical lepidosomes. Nuclear small subunit ribosomal RNA gene and mitochondrial cytochrome oxidase subunit 1 gene sequences place the new genus basal within the order Tetrahymenida, well separated from members of the family Tetrahymenidae (*Lambornella* and *Tetrahymena*) and also from other tetrahymenids (*Colpidium, Dexiostoma, Glaucoma*). The genetic divergences between this species and other genera in Tetrahymenida are large enough to suggest placement of the new genus in a separate family. This corroborates the morphological data, since the elaborate caudal ciliary array and the lepidosome-covered resting cyst of this species are not found in other Tetrahymenidae.

Keywords: Caudal cilia; Cytochrome oxidase subunit 1 gene; *Deltopylum*; Histophagy; Small subunit ribosomal RNA gene; Tetrahymenidae.

Introduction

The family Tetrahymenidae Corliss, 1952 is currently comprised of three genera, *Deltopylum, Lambornella* and *Tetrahymena* (Lynn 2008). *Paraglaucoma* is a junior synonym of *Tetrahymena* (Aescht 2001). *Paratetrahymena* Thompson, 1963 was originally assigned to the family Tetrahymenidae on the basis of morphologic characters (Thompson 1963). Li et al. (2006) established the order Loxocephalida to include *Paratetrahymena*, *Dexiotrichides* and *Cardiostomatella*. Small subunit rRNA (SSrRNA) phylogeny places *Paratetrahymena* outside of the Tetrahymenidae (Yi et al 2009). Lynn (2008) deferred recognition of the order Loxecephalida pending accumulation of additional sequence data and included *Paratetrahymena* in the philasterid family Loxcephalidae Jankowski, 1964. Fauré-Fremiet and Mugard (1946) established the monotypic genus *Deltopylum*. They discovered *D. rhabdoides*, the histophagous type species, in a freshwater stream in France. Diagnostic features of the genus included a triangular buccal overture, sigmoid adoral membranelles and a polytomic mode of division in the non-encysted state. This species has been reported from Poland (Czapik 1968), Germany (Song and Wilbert 1989) and Cameroon (Dragesco and Njiné 1971). The current study describes the morphology, ontogenesis, conjugation and molecular phylogeny of a new polytomically dividing, histophagous tetrahymenid ciliate discovered in a freshwater canal in Boise, Idaho, U.S.A.

Material and Methods

Collection, cultivation and identification

Ciliates were collected from bottom sediments and decaying leaves from a small, slow-flowing freshwater irrigation canal bordering Kathryn Albertson Park in Boise, Idaho (43° 36' 54.93" N; 116° 13' 23.63" W; elev. 817 m). Samples were taken from October through December in 2007 and 2008. Water temperature was about 9.4 °C and pH about 5.9. Samples contained numerous chironomid larvae (Diptera). Raw samples were maintained for up to two weeks at room temperature (20 °C). Cultures were established by placing ciliates selected from raw samples into Petri dishes containing filtered site water. Ciliates were fed with live, wounded chironomid larvae every 3–5

days. Thriving cultures were maintained for up to 10 weeks. The ciliates refused to feed on uninjured larvae, putrefying larvae, or muscle tissue (e.g. chicken or beef). Cultures declined rapidly if unfed for more than five days. The life cycle, morphogenesis and conjugation were studied at intervals after feeding. Live ciliates were studied at magnifications of 40X–1000X with brightfield and differential interference contrast (DIC) using a Zeiss Axioskop 2 plus microscope. The infraciliature was studied using silver impregnation techniques described by Foissner (1991). Resting cysts were examined in wet mounts and India ink suspensions. A Flex digital camera and calibrated Spot imaging software (Diagnostic Instruments, Inc.) were used for microphotography and measurements. In vivo measurements were made from microphotographs of cells in culture dishes to eliminate cover glass compression artifact. Image post-processing was done with Adobe® Photoshop CS4. Statistical analyses were performed using MedCalc for Windows, version 11.2 (MedCalc Software, Mariakerke, Belgium). Drawings were based on microphotographs. Terminology is according to Corliss (1979), Foissner and Xu (2007), Mugard (1949) and Müller et al. (2005). Classification scheme is according to Lynn (2008). We use the term "caudal ciliary array" to describe a discrete group of caudal kinetids (See Discussion).

DNA extraction, amplification and sequencing

DNA was extracted from cells fixed in 80% ethanol using the Chelex method, as modified by Strüder-Kypke and Lynn (2003). Three different samples were processed, adding 50–80 µl of a 5% Chelex 100® solution (Sigma, Oakville, ON, Canada) and 5–8 µl proteinase K (50 mg/ml; Epicentre, Madison, WI, USA) to 10–20 cells, respectively. The RepliG kit (Qiagen, Mississauga, ON, Canada) was used to amplify the extracted DNA in two of the three samples. PCR amplifications of the SSrRNA gene and the mitochondrial cytochrome oxidase subunit 1 (COI) gene were performed in a Gene Amp 2400 thermocycler (PE Applied Biosystems, Mississauga, ON, Canada). Forward primers for the SSrRNA gene were the universal eukaryote primer A (5'-AACCTGGTT-GATCCTGCCAGT-3'; Medlin et al. 1988), and the internal primers 82F (5'-GAAACTGCGAATGGCTC-3'), and 300F (5'-AGGGTTCGATTCCGGAG-3'; Elwood et al. 1985). LSUR (5'-GTTAGTTTCTTTTCCTCCGC-3') was used as the reverse primer. The COI gene was amplified as described in Strüder-Kypke and Lynn (2010), using the forward primer F388dT (5'-TGTAAAACGACGGCCAGTGGWKCBAAAGATGTWGC-3') and the reverse primer R1184dT (5'-CAGGAAACAGCTATGACTADACYTCAGGGTGACCRAAAAATCA-3'). The PCR products were purified with MinElute (Qiagen, Mississauga, ON, Canada) either from a gel, or directly from the PCR reaction. Sequencing in both directions was done with a 3730 DNA Analyzer (Applied Biosystems Inc., Foster City, California, USA), using ABI Prism BigDye Terminator (ver. 3.1) and Cycle Sequencing Ready Reaction kit.

Phylogenetic analyses

All sequences were imported into Sequencher ver. 4.0.5 (Gene Codes Corp.), trimmed at the ends, assembled into contigs, and checked for sequencing errors. The SSrRNA gene sequence was imported into the existing DCSE (Dedicated Comparative Sequence Editor; De Rijk and De Wachter 1993) database and automatically aligned to other hymenostome sequences. Based on the secondary structure of the SSrRNA molecule, we further refined the alignment. The data set used for phylogenetic analyses consisted of 42 species and 1829 positions. The COI sequence was imported into MEGA ver. 4.1 (Kumar et al. 2008), converted into the amino acid sequence and aligned to other hymenostome sequences. The alignment was done by eye and based on the amino acid sequence, due to the great variation between the taxa. A nucleotide data set of 40 species and 750 positions was used in the phylogenetic analyses. Modeltest ver. 3.0 (Posada and Crandall 1998) was employed to find the model of DNA substitution that best fits our data. The General-Time-Reversible (GTR) model for nucleotide substitution was determined as best model, including gamma-distributed substitution rates among sites and considering invariable sites for both genes (SSrRNA and COI). A maximum likelihood analysis was performed using PhyML (Guindon and Gascuel 2003, Guindon et al. 2005) with 500 bootstrap replications. PHYLIP ver. 3.67 (Felsenstein 2005) was employed to calculate genetic distances with the Kimura-2-parameter model (Kimura 1980) using DNADIST. The distance trees were constructed with NEIGHBOR, using the Neighbor Joining (NJ) algorithm (Saitou and Nei 1987). The data were bootstrap re-sampled 1000 times. A maximum parsimony (MP) analysis was performed with PAUP* ver. 4.0b10 (Swofford 2002), using 698 (SSrRNA) and 462 (COI) parsimony-informative characters, respectively. Species were added randomly (n = 5), the tree bisectionreconnection (TBR) branch-swapping algorithm was used, and the data were bootstrap re-sampled 1000 times.

Results

Family Deltopylidae Song and Wilbert, 1989

Remarks: We emend the family diagnosis because the diagnosis of Deltopylidae sensu Song and Wilbert (1989) is likely based on a population other than the type species, *Deltopylum rhabdoides* Fauré-Fremiet and Mugard, 1946 (see Comparison with similar species).

Emended diagnosis: Elongate, histophagous Tetrahymenida; division polytomic in free-swimming state; parallel somatic kineties extending into preoral suture; postoral suture absent; crook-shaped or sigmoid membranelle 1 and membranelle 2 and markedly reduced membranelle 3; tetrahymenid silverline pattern.
Type genus: *Deltopylum* Fauré-Fremiet and Mugard, 1946
Genera assignable: *Deltopylum* Fauré-Fremiet and Mugard, 1946; *Agolohymena* nov. gen.

***Agolohymena* nov. gen.**
Diagnosis: Medium-sized Deltopylidae with multiciliated discoid caudal ciliary array; adoral membranelle 3 vestigial in mature theront; resting cyst covered with tangled tubular or cylindrical lepidosomes.
Type species: *Agolohymena aspidocauda* nov. spec.
Etymology: Composite of the Latin noun *agolum* (shepherd's crook) and the Greek noun *hymen* (membrane), referring to the crook-shaped adoral membranelle 1. Feminine gender.

Description of *Agolohymena aspidocauda* nov. spec. (Figs 1–31, 43–98; Tables 1 and 2)

Diagnosis: Theronts about 150 x 39 µm, trophonts about 154 x 61 µm in vivo. Theronts cylindroidal, bluntly tapered anteriorly, rounded posteriorly. Feeding cells with distinct, rightward-curving rostrum. Trophonts ellipsoidal. Macronucleus strand flattened. Several micronuclei. Single contractile vacuole in right mid-body, two excretory pores. Extrusomes about 3 x 0.6 µm. An average of 88 narrowly spaced ciliary rows, two usually postoral; kineties 3, n-1 and n-2 extend parallel to one another into the preoral suture; dorsolateral kineties commence at a small apical bare area with ciliated dikinetids; discoid caudal ciliary array with an average of 12 kinetids enclosed by a circle of about 20 kinetids. Caudal kinetids individually surrounded by a polygonal silverline. Adoral membranelle 1 sigmoid or crook-shaped; membranelle 2 sigmoid, usually longest; membranelle 3 vestigial; membranelles 1 and 2 each composed of three files of basal bodies. Two kinds of resting cysts: small (about 85 µm) smooth and transparent or large (about 190 µm) with tangled cylindrical or tubular lepidosomes.
Type locality: Freshwater irrigation canal bordering Kathryn Albertson Park in Boise, Idaho, U.S.A. (43° 36' 54.93" N; 116° 13' 23.63" W; elev. 817 m).
Type material: A hapantotype consisting of six protargol-impregnated slides and two dry silver nitrate preparations have been deposited in the Biology Center of the Museum of Natural History of Upper Austria, Linz (LI). Black ink circles on the cover glass mark relevant specimens. SSrRNA and COI gene sequences are available from GenBank under the accession numbers HM014309 and HM01438, respectively.
Etymology: Composite of the Greek noun *aspidos* (small circular shield) and the Latin noun *caudum* (tail) referring to the disc-shaped caudal ciliary array.
Description: Wild and recently cultured theronts about 150 x 39 µm, length:width ratio about 3.9 in vivo; theronts from cultures older than three weeks smaller, ovoid (about 77 x 33 µm); morphostatic theront shape elongate, cylindroidal, slightly curved rightward on long axis, anterior end bluntly tapered, posterior end rounded with slightly oblique truncation. Macronucleus long flattened spiral strand. Five to seven scattered spherical micronuclei (Figs 1, 24–27, 52–54). Multiple macronuclear nodules in exconjugants (Figs 28–30, 96–98). Single contractile vacuole approximately equatorial on right, two excretory pores, one posterior to the other in shallow cortical depression, excretory pores at end of shortened somatic kinety (usually kinety 25). Contractile vacuole with spherical collecting vesicles during diastole, two or more fibrillar bundles (probably microtubules associated with ampullae and spongiome) radiate from each excretory pore in protargol preparations (Figs 1, 13, 43, 44, 49, 62).

Extrusomes peripheral, inconspicuous 3–5 x 0.6 µm, straight or slightly curved rods with rounded ends or narrowly ellipsoidal, perpendicular to cortex, probably mucocyst type, recognizable with DIC in vivo but do not impregnate with silver methods (Figs 4, 50). Cortex relatively inflexible with kineties in shallow narrowly spaced longitudinal furrows (Fig. 49). Cytoplasm hyaline, anterior end of theront appears dark under low magnification due to collection of shiny yellow globules (Figs 51, 72). Cytopyge ventral, subterminal between kinety 1 and kinety n, sometimes visible as pale widened area between kineties in protargol preparations and as argentophilic line in silver nitrate preparations (Fig. 16). Movement of theronts darting, erratic, cell rotates rapidly on long axis, intermittently halts as anterior end describes a large circle with posterior end stationary (Fig. 6); feeding forms avidly attack food source (usually damaged chironomid larvae) in swarms, boring rostrum into exposed tissues (Figs 47, 51); after feeding, trophonts swim more slowly, settle motionless to bottom of culture dish, develop into unencysted tomonts (Figs 45, 72).

Ordinary somatic cilia of uniform diameter, about 8 µm long in vivo. Caudal cilia 12.5–14.5 µm long, stiff, immobile, taper distally (Figs 5, 44, 45, 48). Average of 88 narrowly spaced holotrichous somatic kineties, about 3–4 somatic kineties descend into shallow perioral cortical depression, curve around either side of buccal overture;

usually two (range 1–4) postoral kineties, some occasionally shortened; average of six (range 4– 7) somatic kineties to right of buccal overture with irregular gaps. Somatic kineties occasionally shortened anteriorly; kineties originating at apical bare area commence with ciliated dikinetids. Somatic kineties terminate posteriorly at small circular bare area surrounding caudal ciliary array. Preoral suture convex to left, extends to circular apical bare area. Kinety 3 and kinety n-2 extend along right and left margin of suture respectively, terminate subapically; kinety n-1 extends parallel to kinety n-2 about half the length of preoral suture. Other right and left ventral kineties terminate anteriorly along kinety 3 and kinety n-2 respectively, except about six kineties ending directly on suture between anterior ends of kineties 3 and n-2 and apical bare area. Caudal ciliary array slightly dorsal, consists of 12 (range 7–20) caudal kinetids enclosed by ring of 20 (range 16–27) kinetids (Figs 1, 13–17 , 31, 52–56, 61–65). Regular somatic kineties consist of monokinetids; larger, more densely impregnating granule (probably a parasomal sac) right and anterior of kinetids, usually superimposed over kinetodesma in silver carbonate preparations. Kinetodesmata extend anterior and right of somatic kinetids, often overlap to form densely impregnated kinetodesmal fiber in silver carbonate preparations. Postciliary microtubules may also contribute to this structure (Figs 23, 55, 63). Caudal kinetids larger than somatic kinetids in silver impregnations. Caudal kinetids individually surrounded by argentophilic ring in protargol and silver carbonate preparations (Figs 14, 16, 17, 52, 53, 55, 61, 65).

Buccal overture narrow (about 18 x 7 µm) rounded triangle in shallow subapical depression (Figs 13, 22, 44, 46); buccal cavity larger than overture, broadly funnel-shaped, cytostome at left posterior end; dense irregular argentophilc mass (possibly tangled fibrils) near opening of cytostome in protargol preparations (Figs 52, 56); pharyngeal fibers curl in 2–3 clockwise turns to form concentric circles in protargol preparations (Fig. 57). Three adoral membranelles, contained inside buccal cavity. Long axes of adoral membranelles 1 and 2 directed to left anteriorly. Membranelles 1 and 2 composed of three rows of basal bodies; membranelle 1 ventral to membranelle 2, usually crook-shaped, sometimes sigmoid, proximal part lies on left wall of buccal cavity, anterior part curves sharply reaching right wall; membranelle 2 to right of membranelle 1, sigmoid, anterior end lies inside curve of membranelle 1, proximal end descends deep into buccal cavity, curves strongly left toward cytostome, one or two files of basal bodies shortened distally; membranelle 3 markedly reduced to two short files or miniscule cluster of basal bodies to right of proximal bend of membranelle 2 in theronts, seen only with difficulty even in optimal silver carbonate and protargol-impregnated specimens (Figs 13, 15, 18–22, 52–54, 56–58). Paroral membrane within buccal cavity, stichodyad type, extends along posterior "base" of buccal cavity, consists of two parallel files of tiny basal bodies, outer (right) file ciliated, inner file barren; short fibrils extend from basal bodies of inner file into buccal cavity in silver carbonate impregnations (Figs 18–22, 54, 58).

Feeding cells rapidly become obpyriform with rightward-curving rostrum; rostrum disappears in fully fed trophonts (Figs 45, 47, 51). Trophonts recognizable by slower swimming, broadly ellipsoidal shape (97–202 x 37–97 µm in vivo, usually about 154 x 61 µm, length:width ratio about 2.5), appear dark due to food vacuoles (Figs 2, 45, 51). Tomonts larger than trophonts, lie immobile on bottom of culture vessel (Fig. 72).

Silverline pattern tetrahymenid, intermeridional cross-fibrils extend left between kinetids, distal ends sometimes anastomose with incomplete secondary meridians; isolated secondary silverline meridian at posterior excretory pore of contractile vacuole; caudal kinetids surrounded individually by polygonal silverline. Two radial lines connect each caudal basal body to the polygonal silverline (Figs 16, 59–61).

Resting cysts: Attempts to induce cyst formation in theronts by starvation usually failed. Cells shrank, became vacuolated and died after more than five days of starvation. We found only five encysted cells in a 10-week-old culture. There were two distinct cyst types. Four examples of the first type were small (67–104 µm in diameter) and spherical with a smooth, pliable, transparent membrane. Only one layer was discernible. Small granular globules filled the cytoplasm of the encysted cells and the macronucleus was indistinct. Somatic cilia and the contractile vacuole were still recognizable. Cells excysted immediately when placed under a cover glass (Fig. 66). We found only one example of a larger (188 µm diameter) cyst type. The cyst wall appeared irregular, slightly brownish and opaque, obscuring the enclosed cell. The India ink suspension revealed an outer surface adorned by myriad tortuous intertwined tubular or cylindrical lepidosomes (about 35 µm long and 2.6 µm in diameter). Excystment occurred soon after applying the cover glass. The discrepancy between the cell size and cyst diameter suggests either that the cell only partially filled the inner cavity of the cyst or that the cyst wall was rather thick (Figs 3, 66–69).

Occurrence and ecology: We discovered this new species in bottom detritus of a rocky freshwater irrigation canal bordering Kathryn Albertson Park fed by the Boise River in Boise, Idaho, U.S.A. (43° 36' 54.93" N; 116° 13' 23.63" W; elev. 817 m) from October through December 2007 and 2008. Populations in the canal coincided with the low flow rates of winter months. From April through early October flow increased dramatically, scouring the canal

bottom of detritus and metazoan communities. Food sources (mainly chironomid larvae, but also Ephemeroptera nymphs, oligochaetes, water mites and Planariidae) quickly repopulated the canal during the low flows of winter months coincident with reestablishment of the *A. aspidocauda* population. Given the apparent rarity of cysts, the importance of cyst formation by *A. aspidocauda* in nature is unclear.

Molecular characteristics: The SSrRNA gene sequence of *A. aspidocauda* is 1750 nucleotides long and shows a GC-content of 41%. The amplified region of the mitochondrial COI gene is 803 nucleotides long and has a GC-content of 28%. Both sequences are available from GenBank under the accession numbers HM014309 and HM014308, respectively.

Phylogenetic placement (Figs 99, 100): Both SSrDNA and COI phylogenies place the new genus basal to the families Tetrahymenidae, Glaucomidae, and Turaniellidae in the hymenostome order Tetrahymenida, although this placement is not consistently supported (Figs 99, 100). A comparison of the genetic distances of the tetrahymenid taxa shows distinctly different within-and between-group values for the COI gene: *Agolohymena aspidocauda* differs by 21% (Tetrahymenidae), 22% (Turaniellidae), and 24% (Glaucomidae) from the other families. Likewise, *Glaucoma chattoni* shows divergence values of 19–25% to the other two families. Only the families Turaniellidae and Tetrahymenidae are separated by lower divergence rates of 11–18%. Within these two families, we typically find divergence values of 3–16%.

Ontogenesis (Figs 70–94, Tables 1 and 2)

General aspects: Nearly all individuals in cultures unfed for >24 hours were in the morphostatic theront form. Trophont forms predominated 3–8 hours after feeding. Tomonts and first division tomites predominated 8–16 hours after feeding. Second division tomites and conjugants predominated 16–22 hours after feeding. Division is homothetogenic and polytomic (i.e. rapid sequence of binary fissions) in the free-swimming state. The first division of a tomont (Figs 70a, b) produces two tomites, proter (TIp) and opisthe (TIo). Each of these then rapidly divides (i.e. second division) into two tomites (Figs 70c-e). TIp (i.e. proter of first division) divides into two tomites (proter, TIIp1; opisthe, TIIo1); TIo (i.e. opisthe of first division) also divides into two tomites (proter, TIIp2; opisthe TIIo2). All divisions are isotomic. Stomatogenesis is polyparakinetal. Basal bodies of oral primordia develop from kineties 1 and n. Parental oral structures are completely resorbed. The initial (i.e. abortive) oral primordium of TIIp2 is reabsorbed followed by development of a second oral primordium from which the oral structures are formed (Fig. 86). Of 200 consecutive theronts from a three weekold culture, 75% (149) had ribbon-like macronuclear morphology whereas 25% (51) had multiple macronuclear nodules (see Discussion).

First division: Anterior migration and partial resorption of parental adoral membranelles, paroral membrane and somatic kineties on either side of the buccal overture signal onset of the first division in the tomont (Figs 70, 76–78, 80). Basal body resorption in the parental paroral membrane and adoral membranelles proceeds from proximal to distal. The distal part of membranelle 1 completely resorbs only after completion of the second division. Simultaneously with these morphologic changes, micronuclei align in the region of the division furrow and begin mitosis (Figs 76–78). Before the division furrow appears, new basal bodies proliferate to the left of kineties 1 and n in the middle third of cell to form the initial oral primordium of the opisthe. Shortly after, basal bodies proliferate at the anterior ends of kineties 1 and n posterior to the parental buccal overture forming the oral primordium of the proter (Figs 70, 78, 80). At this stage, there is extensive intrakinetal replication of basal bodies (Figs 63, 81). The macronucleus becomes more compact and less tortuous. Somatic kineties begin to separate at the cell equator. Ends of the macronucleus are drawn out into fine tapered strands anchored to the cortex and the macronucleus divides (Figs 76–79). Micronuclei move to their respective daughter cells before macronuclear karyokinesis begins. A new caudal ciliary array (the future caudal ciliary array of TIIo1) forms from posterior ends of the somatic kineties at the division furrow. Dikinetids appear at the anterior ends of the oral primordia in proter and opisthe (Fig. 79). The proter and opisthe of first division are distinguished in vivo by size, the conical anterior end of the former and slightly truncate posterior end of the latter (Figs 71, 72).

Second division: The second division begins prior to cytokinesis of the first division (i.e. polytomy). Tomites of the second division are distinguishable from tomites of first division in vivo by their smaller size and rounded shape (Figs 70d, e, 72, 74). After TIIo1 and TIIp2 separate, tomites of the second division (TIIp1/TIIo1 and TIIp2/TIIo2) are indistinguishable in vivo. TIIp1 and TIIp2 are distinguishable in silver impregnations by the resorbing membranelle 1 in the former and resorbing initial (i.e. abortive) oral primordium and forming second oral primordium in the latter (Figs 80, 85, 86). Division furrows develop at the equator of TIp and TIo prior to cytokinesis of the first division (Figs 70c, 73). The oral primordium of the "anterior" proter of second division (i.e.

TIIp1) enlarges. The initial oral primordium of TIIp2 migrates anteriorly and degenerates; a new primordium forms just posterior to it (Figs 85, 86). New oral primordia develop in the two opisthes (i.e. TIIo1 and TIIo2). At this stage, four tomites (TIIp1, TIIo1, TIIp2 and TIIo2) are connected in linear fashion (Figs 70c, 73). The fourtomite chain stage persists only briefly since cytokinesis at the first division furrow (i.e. between TIIo1, TIIp2) completes shortly after appearance of the second division furrows. Assembly of adoral membranelles and paroral membrane from the disorganized mono-and dikinetids of the oral primordia proceeds from left anterior to right posterior (i.e. the anterior part of membranelle 1 assembles first and the proximal end of the paroral membrane last). The organization of new adoral membranelles and paroral membrane remains incomplete as tomites of second division separate.

Separated tomites of the second division are broadly ovate. The adoral membranelles each consist of three files of basal bodies parallel to the long axis of the cell. At this stage, the paroral membrane is a "C"-shaped file of obliquely oriented ciliated dikinetids on the right margin of the shallow oval buccal overture. Tomites enlarge and elongate. The distal end of membranelle 3 frays and one of three files of basal bodies resorbs while the remaining two are shortened by resorption at either end. In "young" theronts, membranelle 3 appears as two short files of unciliated basal bodies to the right of membranelle 2. Membranelle 3 remains as only two short files or a tiny cluster of basal bodies in mature theronts. One or two files of basal bodies partly resorb at anterior end of membranelle 2 (Figs 22, 83–94). When resorption of parental oral structures is complete, adoral membranelles 1 and 2 assume a reverse "S" shape. The proximal end of membranelle 1 partially resorbs assuming the "crook" shape characteristic of the mature theront. Membranelle 2 becomes the longest of the adoral membranelles. Membranelles 1 and 2 rotate clockwise. The proximal end of membranelle 2 curves sharply to left and descends into the deepening buccal cavity. Thus, membranelle 2 inclines dorsally in the proximal buccal cavity of the theront. The paroral membrane shortens by resorption of its distal half. The buccal overture assumes the rounded triangle shape characteristic of the theront enclosing the paroral membrane which extends along its proximal "base" (Figs 18–22, 54, 58). The inner file of basal bodies of the paroral membrane loses its cilia. The preoral suture forms in all four tomites by anterior elongation of kinety 3 on its right and kineties n-1 and n-2 on its left (Figs 92, 93).

The new caudal ciliary array of TIIo1 fully forms shortly after cytokinesis of the first division. TIIp1 and TIIp2 each develop a new caudal ciliary array. TIIo2 retains the parental caudal ciliary array. New caudal ciliary arrays, derived from the posterior ends of ventral somatic kineties at the division furrow, are completely formed soon after tomites separate (Figs 79, 91).

The macronucleus lengthens into a flattened spiral ribbon after the second division tomites separate. After cytokinesis of the second division, tomites rapidly elongate and transform into theronts. Some tomites of second division have three contractile vacuole pores one of which is lost in the theront. Food vacuoles and/or cytoplasmic glycogen globules are consumed during the first division. During the first and second division, cells usually remain motionless in a thin layer of mucus but swim away rapidly if disturbed.

Conjugation (Figs 95–98, Tables 1 and 2)

Many conjugants are found in 2-3 week-old cultures. Conjugation occurs between second division tomites. Conjugation is isopolar and anisogamic. Conjugants show a small but significant difference in length (Table 1; median length 70.0 vs. 63.3 µm, $p < 0.05$). Exconjugants are ovate to reniform and their anterior ends often taper to a short point. Oral structures are reduced to patches of basal bodies at the proximal end of a subapical furrow. Conjugants show patchy loss of somatic kinetids and the caudal ciliary array appears very small and condensed in protargol-impregnated specimens. The macronuclei of conjugants and recent exconjugants are contracted, lobulated and hyperchromatic. The macronucleus degenerates in exconjugants and reforms from numerous anlagen derived from postgamic micronuclear divisions (Figs 96–98).

Discussion

The caudal ciliary array

Morphologic and molecular data clearly place *Agolohymena* in the order Tetrahymenida. However, *A. aspidocauda* has a caudal ciliary array not found in other members of the family Tetrahymenidae. The terminology of caudal ciliary structures is somewhat vague. Holz and Corliss (1956) used the term "polar basal granule-complex" to describe a single caudal kinetosome and its associated silverlines in *Tetrahymena setifera* Holz and Corliss, 1956. However, Thompson and Berger (1959) referred to the same structure as a "polar basal body complex" (PBB-complex). Corliss (1979) defined the "polar-basal-body complex" as a single "...infraciliary kinetosome, bearing a long and often stiff caudal cilium, plus a pair of parasomal sacs". Lynn (2008) defined the PBB-complex as a "grouping of kinetosomes and sometimes parasomal sacs... ." Because the word "complex" has been used to refer to

both single and multiple kinetids, we prefer the term "caudal ciliary array" to describe a distinct group of caudal kinetids. Several histophagous species of *Tetrahymena* (*T. corlissi*, *T. bergeri*, *T. rostrata* and *T. setosa*) possess a single caudal cilium but no other Tetrahymenidae have discoid or ring-like caudal ciliary arrays (Corliss 1970). Both genera of the tetrahymenid family Spirozonidae (i.e. *Spirozona* and *Stegochilum*) have circular or ring-like caudal ciliary arrays that are structurally simpler than that of *A. aspidocauda*. In spirozonid species, the caudal basal bodies each lie on a primary somatic ciliary meridian and are not surrounded by a silverline ring in silver nitrate preparations (Foissner 1986). *Trichospira inversa*, type species of the only genus in the tetrahymenid family Trichospiridae, has a tuft of caudal cilia but they are not arranged in a circular caudal ciliary array (Jankowski 1964; Klein 1930). The discoid caudal ciliary array of *A. aspidocauda* is unique among the Tetrahymenida in its complexity. The cilia of this array are morphologically and functionally distinct from other somatic cilia and the kinetids are morphologically distinct from ordinary somatic kinetids in silver carbonate, protargol and silver nitrate-impregnated specimens. In *A. aspidocauda*, each caudal kinetid is a "polar basal granule-complex" sensu Holz and Corliss (1956) i.e. "this complex …appears to be composed either of more than one granule or of an enlarged granule typically tripartite in nature. The argentophilic granular structure is usually more or less completely encircled, at a short radius, by a delicate fibril which isolates the granule(s)...". Single polar basal granule complexes have been described in scuticociliates (Kaneshiro and Holz 1976) and some tetrahymenids (Foissner 2003). These caudal kinetids, like those of *A. aspidocauda*, appear unusually large in silver preparations probably due to silver deposition at junctions between pellicular alveoli and parasomal sacs surrounding the kinetosome. The kinetosome itself is indistinguishable (at least in *Uronema* species) from that of ordinary somatic kinetids by electron microscopy (Kaneshiro and Holz 1976; Pitelka 1961). The caudal cilia of *A. aspidocauda* show similar modifications (i.e. immobility, increased length and distal tapering) to those of the caudal cilium in *Tetrahymena setosa*, *Lambornella trichoglossa* and the philasterine scuticociliate genus *Uronema* (Foissner 2003; Holz and Corliss 1956; Kaneshiro and Holz 1976). The proximal microtubular structure of the caudal cilium is unremarkable on transmission electron microscopy (Kaneshiro and Holz 1976). Although often assumed to be thigmotactic, the functional role of these modified cilia is still unknown.

Macronuclear morphology

The macronuclear morphology of *D. rhabdoides* is somewhat puzzling (Dragesco and Njiné 1971). Fauré-Fremiet and Mugard (1946) and Mugard and Lorsignol (1956) stated that the ribbon-like macronucleus of *D. rhabdoides* normally dissociated into multiple nodules in "young" theronts and that these nodules reassociated into the ribbon-like form prior to division. Dragesco and Njiné (1971) reported invariably multinodular macronuclei in *D. rhabdoides*. In *A. aspidocauda* (and probably *D. rhabdoides*), multiple macronuclear nodules most likely represent macronuclear anlagen of exconjugants. Fauré-Fremiet and Mugard (1946) found only one pair of conjugants in *D. rhabdoides* and provided no details. Although some general observations on conjugation in *A. aspidocauda* are provided in the current report, details of the complex nuclear events of conjugation and morphologic development of exconjugants in this multimicronucleate species remain largely unknown and require further study.

Resting cysts

Observations on resting cysts of *A. aspidocauda* must be interpreted with caution since we found only five examples. We did not determine the chemical composition of the tangled structures coating the resting cyst of *A. aspidocauda*, however they are likely organic rather than siliceous and thus we refer to them as lepidosomes (Müller et al. 2005). The finding of tubular or cylindrical lepidosomes requires confirmation, preferably by electron microscopy and chemical characterization of these structures. Lepidosome-coated resting cysts have not been reported in other Tetrahymenidae.

Comparison with similar species

The morphologic features of *A. aspidocauda* (e.g. size and shape of adoral membranelles and the paroral membrane, number of excretory pores) vary significantly according to the stages of its life cycle. Following the convention established for *D.*
rhabdoides by Fauré-Fremiet and Mugard (1946), the current report bases the species diagnosis on the morphology of the theront.

Agolohymena aspidocauda, especially its rostrate feeding form (Figs 11, 47), may be confused with *Ophryoglena* species at low magnification in vivo. However, the theront is clearly distinguishable from *Ophryoglena* by its slender cylindroidal shape vs. the more fusiform shape of *Ophryoglena* species, absence of Lieberkühn's organelle and division in the unencysted state vs. division in cysts in *Ophryoglena* species (Lynn 2008; Lynn et al. 1991).

The morphologic and ontogenetic features of *A. aspidocauda* are quite similar to those of *Deltopylum rhabdoides* (Fauré-Fremiet and Mugard 1946; Mugard 1949; Mugard and Lorsignol 1956). Fauré-Fremiet and Mugard (1946) and Czapik (1968) found *D. rhabdoides* in freshwater streams of France and Poland during winter months. The depiction of the preoral suture (Fig. 32) is somewhat unclear (i.e. kinety 3 and kinety n-1 are depicted as merging, giving the misimpression that kinety n-1 rather than kinety 3 forms the right side of the suture whereas kinety n-1 probably terminates in the proximal part of the suture as in *A. aspidocauda*). The suture differs slightly from that of *A. aspidocauda* (kinety 3 and kinety n-2 extend to the anterior pole vs. kinety 3 and kinety n-2 terminating proximal to the apical bare area in *A. aspidocauda*). Fauré-Fremiet (1969) noted that Czapik's (1968) description of *D. rhabdoides* was based on observations of tomites rather than the theront form. He concurred with her finding of only two files of basal bodies in all adoral membranelles. It is likely that this observation was erroneous. In *A. aspidocauda* the adoral membranelles (prior to regression of membranelle 3) are all composed of three files of basal bodies. Fauré-Fremiet clearly showed a regression of membranelle 3 to two short files of basal bodies in *D. rhabdoides*, identical to the findings in *A. aspidocauda* (Figs 32, 34–37). The discoid caudal ciliary array is the main morphologic feature distinguishing *A. aspidocauda* from *D. rhabdoides*. Fauré-Fremiet and Mugard (1946) stated that *D. rhabdoides* "never" formed cysts but *Agolohymena aspidocauda* appears to form two types of resting cysts, one form covered with unusual lepidosomes. The ontogenesis of *A. aspidocauda* conforms, with the exceptions noted above, to that of *D. rhabdoides* so carefully described by Fauré-Fremiet and Mugard (1946), Mugard (1949) and Mugard and Lorsignol (1956).

Song and Wilbert (1989) identified a ciliate from the Botanic Garden pond in Bonn, Germany as *D. rhabdoides* (Figs 39–42). They established the family Deltopylidae in the order Tetrahymenida and based the diagnosis of this family, in part, on a lattice-like peniculine silverline system ("…indirekt verbindendes Silberliniensystem gitterförmig (*Paramecium*-ähnlich)"). They also included the silverline system as a diagnostic feature of the genus *Deltopylum* (Fig. 41). Recognizing the discrepancy with the silverline system of other members of the suborder Tetrahymenina Fauré-Fremiet in Corliss, 1956, they considered emending the definition of Tetrahymenina or placing Deltopylidae in a new suborder. The somatic infraciliature and buccal apparatus of the population described by Song and Wilbert (1989) are quite different from those of both *D. rhabdoides* Fauré-Fremiet and Mugard, 1946 and *A. aspidocauda*. Their population had 6–7 postoral kineties vs. 2–4 in *D. rhabdoides* and 1–4 in *A. aspidocauda*. Right and left somatic kineties met end-to-end along a straight preoral suture vs. extension of somatic kineties into the preoral suture in *D. rhabdoides* and *A. aspidocauda*. The somatic kineties did not commence with dikinetids. The three adoral membranelles were all approximately the same length and relatively straight vs. crook-shaped/sigmoid membranelle 1 and membranelle 2 and miniscule membranelle 3 in *D. rhabdoides* and *A. aspidocauda*. The paroral membrane was longitudinally oriented and extended further anteriorly than in *D. rhabdoides* or *A. aspidocauda* (Fig. 42). Fauré-Fremiet and Mugard (1946) did not describe the silverline pattern of *D. rhabdoides*. Based on these discrepancies, we conclude that *D. rhabdoides* sensu Song and Wilbert (1989) is a misidentification and belongs to a genus other than *Deltopylum* and that a lattice-like (i.e. peniculine) silverline system is not a feature of the genus *Deltopylum*.

Dragesco and Njiné (1971) described a population of *D. rhabdoides* from Cameroon (Fig. 33). They ascribed the variability of adoral membranelle size and macronuclear morphology in their population to differences in life cycle stages. The preoral suture of their population differs from that of *A. aspidocauda* (i.e. the anterior ends of kinety n-2 through kinety n-10 terminate on kinety 2 which extends into the preoral suture). The macronucleus was invariably multinodular. Macronuclear nodules of the African population were smaller (mean diameter 2.4 µm vs. 5.6 µm) and more numerous (mean number 95 vs. 27) than those found in exconjugants of *A. aspidocauda*. Mugard and Lorsignol (1956) also found fewer, larger macronuclear nodules in their European population of *D. rhabdoides*. Adoral membranelle 3 was longer than membranelle 2 in the African *D. rhabdoides*. This conflicts with the illustrations of Fauré-Fremiet and Mugard (1946) and Fauré-Fremiet (1969). Adoral membranelle 3 is invariably vestigial in theronts of *A. aspidocauda* and is invariably the shortest of the three adoral membranelles during all stages of stomatogenesis. The African population lacked caudal cilia. The preoral suture also differed from that of the type population of *D. rhabdoides* Fauré-Fremiet and Mugard, 1946 (i.e. only kinety 2 and kinety n-2 extended into the preoral suture). These morphologic differences and its tropical habitat suggest that the ciliate described by Dragesco and Njiné (1971) may represent a second species of *Deltopylum*.

Foissner (2003) described a large tetrahymenid, *Lambornella trichoglossa*, from the tanks of bromeliads in Brazil and the Dominican Republic. He acknowledged the uncertainty of the generic classification noting that his population did not form cuticular cysts on mosquito larvae, a main generic character for *Lambornella* (Corliss and

Coats 1976). Based on SSrDNA sequences, Lynn (2008) and Strüder-Kypke et al. (2001) suggest that *Lambornella* is probably a junior synonym of *Tetrahymena*. Foissner's species had sigmoid adoral organelles, a reduced membranelle 3 and at least partial reorganization of parental oral structures during ontogenesis. This species is easily distinguished from *A. aspidocauda* by its more or less distinct tail, an omnivorous mode of nutrition, a spherical macronucleus, a single micronucleus, a silverline pattern of prominent loop-shaped intermeridional cross-fibrils, a single caudal cilium, a nonpolytomic mode of division and its habitat (i.e. the tanks of bromeliads).

Systematic position of *Agolohymena aspidocauda*

The molecular phylogenetic analyses support our morphological observations. *Agolohymena aspidocauda* does not branch within the family Tetrahymenidae, but rather basal to it (Figs 99, 100). ML and MP analyses of the SSrRNA gene show considerable support (90% ML, 81% MP) for a placement basal to the families Tetrahymenidae, Glaucomidae, and Turaniellidae. The NJ analysis, however, prefers a sister-group relationship between *A. aspidocauda* and species of the family Tetrahymenidae (58% vs. 33%; data not shown). The phylogenetic analyses of the COI gene also group *A. aspidocauda* basal to the other three families, however, with much lower support (66% ML, 65% NJ, 22% MP). This is partly due to the restricted capability of COI gene phylogenies to resolve the relationships of distantly related taxa (Strüder-Kypke and Lynn 2010). The comparison of the genetic distances of the COI gene within (3–16%) and between (19–25%) families of the Tetrahymenida supports the placement of *A. aspidocauda* in a separate family. Clearly, more taxa need to be sequenced, and especially a sequence of *Deltopylum* is needed to fully confirm our conclusions.

Acknowledgements

We are greatly indebted to Professor Wilhelm Foissner (University of Salzburg) for his kind encouragement and thoughtful critique. Dr. Denis Lynn (University of Guelph) generously provided important taxonomic advice and funded the molecular work of MSK through an NSERC Discovery Grant.

References

Aescht, E., 2001. Catalogue of the generic names of ciliates (Protozoa, Ciliophora). Denisia 1, 1–350. Corliss, J.O., 1970. The comparative systematics of species comprising the hymenostome ciliate genus *Tetrahymena*. J. Protozool. 17, 198–209. Corliss, J.O., 1979. The Ciliated Protozoa: Characterization, Classification and Guide to the Literature, 2nd ed. Pergamon Press, Oxford, New York.

Corliss, J.O., Coats, D.W., 1976. A new cuticular cyst-producing tetrahymenid ciliate, *Lambornella clarki* n. sp., and the current status of ciliatosis in culicine mosquitoes. Trans. Am. Microsc. Soc. 95, 725–739.

Czapik, A., 1968. Remarques sur *Deltopylum rhabdoides* Fauré-Fremiet et Mugard (Ciliata, Hymenostomata). Acta Protozool. 6, 57–58.

De Rijk, P., De Wachter, R., 1993. DCSE, an interactive tool for sequence alignment and secondary structure research. CABIOS 9, 735–740.

Dragesco, J., Njiné, T., 1971. Compléments à la connaisance des Ciliés libres de Cameroun. Ann. Fac. Sci. Cameroun 7 and 8, 97–140.

Elwood, H., Olsen, G., Sogin, M., 1985. The small-subunit ribosomal RNA gene sequences from the hypotrichous ciliates *Oxytricha nova* and *Stylonychia pustulata*. Mol. Biol. Evol. 2, 399–410.

Fauré-Fremiet, E., 1969. A propos de *Deltopylum rhabdoides*. Acta Protozool. 7, 25–27.

Fauré-Fremiet, E., Mugard, H., 1946. Sur un infusoire holotriche histiophage *Deltopylum rhabdoides*, n. gen., n. sp. Bull. Soc. Zool. Fr. 71, 161–164.

Felsenstein, J., 2005. PHYLIP (Phylogeny Inference Package) version 3.6a2. 3.65 ed. Seattle, Washington, Distributed by the author, Dept. of Genetics, University of Washington.

Foissner, W., 1986. Revision der Gattung *Stegochilum* Schewiakoff, 1892. Acta

Protozool. 25, 1–14.

Foissner, W., 1991. Basic light and scanning electron microscopic methods for taxonomic studies of ciliated protozoa. Eur. J. Protistol. 27, 313–330.

Foissner, W., 2003. Morphology and ontogenesis of *Lambornella trichoglossa* nov. spec., a new tetrahymenid ciliate (Protozoa, Ciliophora) from Brasilian tank bromeliads (Bromeliaceae). Eur. J. Protistol. 39, 63–82.

Foissner, W., Xu, K., 2007. Monograph of the Spathidiida (Ciliophora, Haptoria). Vol. I: Protospathidiidae, Arcuospathidiidae, Apertospathulidae. Monogr. Biol. 81, 1–485.

Guindon, S., Gascuel, O., 2003. A simple, fast and accurate algorithm to estimate large phylogenies by maximum likelihood. Syst. Biol. 52, 696–704.

Guindon, S., Lethiec, F., Duroux, P., Gascuel, O., 2005. PhyML Online -a web server for fast maximum likelihood-based phylogenetic inference. Nucl. Acids Res. 33, W557–559.

Holz, G.G., Corliss, J.O., 1956. *Tetrahymena setifera* n. sp., a member of the genus *Tetrahymena* with a caudal cilium. J. Protozool. 3, 112–118.

Jankowski, A.W., 1964. Morphology and evolution of Ciliophora. III. Diagnoses and phylogenies of 53 sapropelobionts, mainly of the order Heterotrichida. Arch. Protistenk. 107, 185–294.

Kaneshiro, E., Holz, G.G., 1976. Observations on the ultrastructure of *Uronema* spp., marine scuticociliates. J. Protozool. 23, 503–517.

Kimura, M., 1980. A simple model for estimating evolutionary rates of base substitutions through comparative studies of nucleotide sequences. J. Mol. Evol. 16, 111–120.

Klein, B.M., 1930. Das Silberliniensystem der Ciliaten. Weitere Ergebnisse. IV. Arch. Protistenk. 69, 235–326.

Kumar, S., Nei, M., Dudley, J., Tamura, K., 2008. MEGA: a biologist-centric software for evolutionary analysis of DNA and protein sequences. Briefings in Bioinformatics 9, 299–306.

Li, L., Song, W., Warren, A., Wang, Y., Ma, H., Hu, X., Chen, Z., 2006. Phylogenetic position of the marine ciliate, *Cardiostomatella vermiforme* (Kahl, 1928) Corliss, 1960 inferred from the complete SSrRNA gene sequence, with establishment of a new order Loxocephalida n. ord. (Ciliophora, Oligohymenophorea). Eur. J. Protistol. 42, 107–14.

Lynn, D.H., 2008. The Ciliated Protozoa: Characterization, Classification and Guide to the Literature, 3rd ed. Springer, Dordrecht.

Lynn, D.H., Frombach, S., Ewing, M., Kocan, K., 1991. The organelle of Lieberkühn as a synapomorphy for the Ophryoglenina (Ciliophora: Hymenostomatida). Trans. Am. Microsc. Soc. 110, 1–l 1.

Medlin, L.K., Elwood, H.J., Stickel, S., Sogin, M.L., 1988. The characterization of enzymatically amplified eukaryotic 16S-like rRNA-coding regions. Gene 71, 491–499.

Mugard, H., 1949. Contributions à l'étude des infusoires hyménostomes histiophages. Ann. Sci. Nat. Zool. Biol. An. (Série 11) 10 (year 1948), 171–271.

Mugard, H., Lorsignol, L., 1956. Étude de la division et de la régénération chez deux Ophryoglenidae d'eau douce: *Ophryoglena pectans* et *Deltopylum rhabdoides*. Bull. Biol. Fr. Belg. 90, 446–464.

Müller, H., Foissner, W., Weisse, T., 2005. The unusual, lepidosome-coated resting cyst of *Meseres corlissi* (Ciliophora: Oligotrichea): Light and scanning electron microscopy, cytochemistry. Acta Protozool. 44, 201–215.

Pitelka, D., 1961. Fine structure of the silverline and fibrillar systems of three

tetrahymenid ciliates. J. Protozool. 8, 75–89.

Posada, D., Crandall, K., 1998. MODELTEST: testing the model of DNA substitution. Bioinformatics 14, 817–818.

Saitou, N., Nei, M., 1987. The neighbor-joining method: a new method for reconstructing phylogenetic trees. Mol. Biol. Evol. 4, 406–425.

Song, W., Wilbert, N., 1989. Taxonomische Untersuchungen an Aufwuchsciliaten (Protozoa, Ciliophora) im Poppelsdorfer Weiher, Bonn. Lauterbornia 3, 1–221.

Strüder-Kypke, M.C., Lynn, D.H., 2003. Sequence analyses of the small subunit rRNA gene confirm the paraphyly of oligotrich ciliates *sensu lato* and support the monophyly of the subclasses Oligotrichia and Choreotrichia (Ciliophora, Spirotrichea). J. Zool. Lond. 260, 87–97.

Strüder-Kypke, M.C., Lynn, D.H., 2010. Comparative analysis of the mitochondrial cytochrome c oxidase subunit I (COI) gene in ciliates (Alveolata, Ciliophora) and evaluation of its suitability as a marker for barcoding. Syst. Biodiv. 8, 131–148.

Strüder-Kypke, M.C., Wright, A.D., Jerome, C., Lynn, D.H., 2001. Parallel evolution of histophagy in ciliates of the genus *Tetrahymena*. BMC Evol. Biol., http://www.biomedcentral.com/1471–2148/1/5.

Swofford, D., 2002. PAUP*: Phylogenetic analysis using parsimony. 4.0b10 ed. Sunderland, Massachusetts, Sinauer.

Thompson, J. C., Berger, J., 1959. *Paranophrys marina* n. g., n. sp., a new ciliate associated with a hydroid from the Northeast Pacific (Ciliata: Hymenostomatida). J. Protozool. 12, 527–531.

Thompson, J. C., 1963. The generic significance of the buccal infraciliature in the family Tetrahymenidae and a proposed new genus and species, *Paratetrahymena wassi*. Va. J.

Sci. 14, 126–135.

Yi, Z., Song, W., Gong, J., Warren, A., Al-Rasheid, K., Al-Arifi, S., Al-Khedhairy, A., 2009. Phylogeny of six oligohymenophoreans (Protozoa, Ciliophora) inferred from small subunit rRNA gene sequences. Zoologica Scripta 38, 323–331.

Figs 1–12. *Agolohymena aspidocauda* from life (1, 2, 4–12) and India ink suspension (3). **1.** Theront, ventral view. **2.** Trophont, ventral view. **3.** Lepidosome-covered resting cyst. **4.** Variable shape of extrusomes. **5.** Caudal cilia. **6.** Theront swimming pattern. **7–12.** Cell outlines, theront (7–10), rostrate feeding form (11), trophont (12). CC, caudal cilia; L, lepidosomes; SC, ordinary somatic cilia. Scale bars 50 µm (3), 25 µm (1, 2, 7–12), 2 µm (4, 5).

Figs 13–31. *Agolohymena aspidocauda* after protargol (13–15, 17, 24–31), dry silver nitrate (16) and silver carbonate (18–23) impregnation. **13.** Ventral infraciliature. **14.** Dorsal. **15.** Anterior infraciliature. **16.** Caudal silverline pattern. **17.** Caudal ciliary array. **18–22.** Variations in oral infraciliature. **23.** Somatic kinety. **24–27.** Mature theront macronuclear morphology. **28.** Exconjugant macronuclear reorganization. **29, 30.** Multinodular macronuclei in exconjugants. **31.** Anterior pole infraciliature. BO, buccal overture; CA, caudal ciliary array; Cy, cytopyge; DK, dikinetids; EP, excretory pores; K3, Kinety 3; Kd, kinetodesma; Kn, Kinety n; Kn-2, Kinety n-2; KS, kinetosome; M1M3, adoral membranelles 1–3; Ma, macronucleus; Mi, micronuclei; PM, paroral membrane; PS, parasomal sac; S, preoral suture; SK, somatic kinetids. Scale bars 25 µm (13–15, 24–30), 10 µm (16–22, 31) and 2 µm (23).

Figs 32–42. *Deltopylum rhabdoides* after unspecified silver impregnation (32, 34–38), from life (39), after protargol (33, 40, 42) and silver nitrate (41) impregnation. **32.** Ventral view (from Fauré-Fremiet and Mugard 1946). **33.** Multinodular macronucleus, ventral view (from Dragesco and Njiné 1971). **34–38.** Variations of buccal apparatus. Figs 34, 35 and 38 probably represent developing second division tomites (34–37 from Fauré-Fremiet 1969; 38 from Dragesco and Njiné 1971). **39–42.** Ventral view (39). Multinodular macronucleus and excretory pores (40). Peniculine silverline pattern (41, size not given). Somatic and buccal infraciliature (42, size not given), ventral view (from Song and Wilbert 1989). CV, contractile vacuole; DiSS, "direct" silverlines (i.e. primary meridians); IdSS, "indirect" silverlines (i.e. secondary meridians); Ma,

macronucleus; Mi, micronucleus; mo, paroral membrane; M1–M3 and m1 –m3, adoral membranelles 1– 3; PM, paroral membrane. Scale bars 50 μm (32, 33, 39, 40), 10 μm (34–38).

Figs 43–51. *Agolohymena aspidocauda* from life (43–46, 48–50 DIC; 47, 51 brightfield).

43. Theront, ventral view. Buccal overture (white arrowhead); contractile vacuole (black arrowhead). **44.** Theront, right lateral view. Cortical depression at buccal overture (arrow); collecting vesicles of contractile vacuole (arrowheads). **45.** Trophont, ventral view; caudal cilia (arrow). **46.** Buccal overture. **47.** Feeding forms with rostra. **48.** Caudal cilia (white arrowheads); ordinary somatic cilium (black arrowhead). **49.** Excretory pores (white arrowhead), right lateral view. **50.** Extrusomes (arrowheads). **51.** Theronts devouring injured chironomid larva (asterisk). Scale bars 200 μm (51), 50 μm (47), 25 μm (43–45), 10 μm (46, 48–50).

Figs 52–60. *Agolohymena aspidocauda* after protargol (52, 53, 56, 57), silver carbonate (54, 55, 58) and dry silver nitrate (59, 60) impregnation. **52.** Infraciliature, left ventrolateral view. Dense mass of fibrils near the cytostome (arrow); micronuclei (black arrowheads). **53.** Infraciliature, right dorsolateral view. Excretory pores with radiating fibrils (white arrowhead). **54.** Buccal apparatus, ventral view; gaps in somatic kineties to right of buccal overture (arrowhead); paroral membrane (arrow). **55**. Caudal ciliary array; kinetodesma (arrow). **56.** Buccal apparatus, preoral suture, anterior bare area, dense fibrils near the cytostome (arrow), right ventrolateral view. **57.** Curled cytopharyngeal fibers (white arrowhead); buccal apparatus (black arrowhead), ventral view. **58.** Buccal apparatus. **59, 60.** Silverline pattern, ventral (59); anterolateral (60). CA, caudal ciliary array; K, kinetid; Ma, macronucleus; M1–3, adoral membranelles 1–3; PM, paroral membrane; PrM, primary meridian; SM, secondary meridian; T, transverse intermeridional fibrils. Scale bars 25 μm (52–54, 56, 57), 10 μm (55, 58–60).

Figs 61–69. *Agolohymena aspidocauda* after dry silver nitrate (61), protargol (62, 64, 65) and silver carbonate impregnation (63), from life (66) and India ink suspension (67–69).

61. Caudal ciliary array silverline pattern (arrowheads). **62.** Excretory pores (arrows), fibrils (arrowheads) of contractile vacuole. **63.** Somatic kineties, ventrolateral; newly replicated kinetosomes (arrowheads). **64.** Preoral suture (arrow); bare area bordered by dikinetids (arrowheads), right lateral view. **65.** Caudal ciliary array, terminal cluster (black arrowhead) and surrounding ring (white arrowhead) of kinetids. **66.** Resting cysts, small clear form; compression of excysting cell by transparent cyst wall (arrowheads); intact cyst (arrow). **67.** Resting cyst, large lepidosome-covered form (arrow); excysted cell (black arrowhead) has just escaped through breach in cyst wall (white arrowhead).

68. Lepidosomes (arrowheads) on surface of large resting cyst. **69.** Detached lepidosomes. K, kinetosomes; Kd, kinetodesma; PS, parasomal sac. Scale bars 50 µm (67), 25 µm (66, 68, 69), 10µm (61–65). **Fig. 70.** *Agolohymena aspidocauda*, schematic of division. First division (a, b). Second division (c–e). Cytokinesis of first (d) and second (e) divisions. CA, caudal ciliary array; K1, Kinety 1; Kn, Kinety n; M1, adoral membranelle 1; OP, oral primordium (stomatogenic field); PM, paroral membrane; ROS, resorbing parental oral structures; TIp, proter of first division; TIo, opisthe of first division; TIIp1, "anterior" proter of second division; TIIp2, "posterior" proter of second division; TIIo1, "anterior" opisthe of second division; TIIo2, "posterior" opisthe of second division. **Figs 71–75.** *Agolohymena aspidocauda* from life (brightfield). **71.** Tomites prior to first division cytokinesis (black arrowheads); tomites after completion of first division cytokinesis (white arrowheads) developing second division furrow. **72.** Theront (white arrow), tomonts (black arrows); tomites before (black arrowhead) and after (white arrowheads) second division cytokinesis. **73.** Tomites just prior to first division cytokinesis forming second division furrows (arrowheads). **74.** First division tomites (black arrowheads) prior to cytokinesis; tomites of second division (white arrowheads) prior to second division cytokinesis. **75.** Anisogamic

conjugants (black arrowheads). Scale bars 100 μm (71), 50 μm (72–75). **Figs 76–82.** Ontogenesis of *Agolohymena aspidocauda* after protargol (76–79, 82) and silver carbonate (80, 81) impregnation. **76.** Tomont, early stage of first division; anaphase micronuclei (black arrowheads) align near division furrow (asterisks); resorbing parental buccal apparatus (arrow). **77.** Slightly later stage of first division; ends of elongating macronucleus drawn into tapering processes (white arrowheads) anchored to cortex. Oral primordium (white arrow); micronuclei entering telophase (black arrowheads); first division furrow (asterisks); caudal ciliary array (black arrow). **78.** Oral primordia in the proter (white arrow) and opisthe (black arrow) of first division; micronuclei completing first division (white arrowheads); micronucleus undergoing second division (black arrowheads), first macronuclear division still incomplete. **79.** Later stage of first division, macronuclear karyokinesis nearly complete; cluster of basal bodies near division furrow (white arrowhead) forms caudal ciliary array of "anterior opisthe" (TIIo1) of second division. **80.** Early stage of stomatogenesis in proter of first division (TIp). Resorbing parental adoral organelles (M1, black arrowhead; M2, white arrowhead); oral primordium forms from kineties 1 and n (asterisk); somatic kineties forming preoral suture (arrows) disorganize and reform during stomatogenesis. **81.** Basal bodies arising from kineties 1 and n (black arrowheads) form oral primordium of opisthe of first division (TIo) near division furrow (asterisks). **82.** Tomite beginning second division. Anaphase micronuclei (arrowheads) align near future division furrow. Ma, macronucleus. Scale bars 25 μm (76– 79, 82), 10 μm (80, 81). **Figs 83–94.** *Agolohymena aspidocauda* after silver carbonate (83, 84, 87, 94) and protargol impregnation (85, 86, 88–93). **83.** First division proter starting second division (see Fig. 70c). Initial TIIp2 oral primordium (black arrowhead) forms from two stomatogenic kineties near division furrow (asterisks); oral primordium (white arrowhead) of TIIp1; parental M1 (arrow) is resorbing. **84.** Middle stage

of second division (TIIp1/TIIo1) after first cytokinesis, oral primordia expand (arrowheads); paroral membrane formation has not started; caudal ciliary array of TIIo1 is assembling (arrow). **85.** Second division tomites (TIIp2/TIIo2). Initial oral primordium resorbs (arrow) as second oral primordium of TIIp2 (black arrowhead) forms; oral primordium of TIIo2 (white arrowhead) develops at division furrow. **86.** Stomatogenesis of TIIp2 during second division. Initial (i.e. abortive) oral primordium resorbs (black arrowhead); second primordium (white arrowhead) arises from two stomatogenic kineties. **87.** Second division. Mono-and dikinetids of oral primordia assemble into adoral membranelles (white arrowhead). **88.** Second division stomatogenesis. Adoral membranelles consist of 3 files of basal bodies (white arrowheads). **89.** Paroral membrane (white arrowhead) organizes from distal to proximal; adoral membranelles (black arrowhead) organize distal to proximal and left to right; asterisk marks developing preoral suture. **90.** Middle stage of second division stomatogenesis. Adoral membranelle formation nearly complete; posterior paroral membrane (white arrowhead) assembly continues. **91.** Second division. As oral structures (black arrowheads) organize, kinetids for proter caudal ciliary array (white arrowhead) separate from posterior left somatic kineties of proter at division furrow. Arrow indicates opisthe caudal ciliary array. Anterior end of M1 curves to right. **92.** Late stomatogenesis after second division cytokinesis. Paroral membrane (arrow) consists of dikinetids; anterior end of M3 (black arrowhead) frays and resorbs; inner one or two files (white arrowhead) of distal M2 resorb. **93.** Late stomatogenesis after second division cytokinesis. M3 (black arrowhead) reduced to two short files. K3, Kn-1 and Kn2 extend to form preoral suture (white arrowhead). **94.** Buccal apparatus (squashed specimen). Distal end M1 (arrow), proximal part M2 (black arrowhead); M3 reduced to two inconspicuous files and small cluster of basal bodies (white arrowhead). Scale bars 25 μm (83–93), 10 μm (94).

Figs 95–98. *Agolohymena aspidocauda* conjugants (95) and exconjugants (96–98) after protargol impregnation. **95.** Anisogamic conjugants. Micronuclei (white arrowheads) beginning pregamic division; reduced, disorganized buccal apparatus (arrow); condensed caudal ciliary arrays (black arrowheads). **96.** Recent exconjugant. Buccal apparatus (black arrowhead) reduced to clusters of basal bodies at posterior end of subapical furrow (arrow); macronuclear anlagen (white arrowheads) visible. **97.** Exconjugant. Micronuclei undergo postgamic division (white arrowheads) as macronucleus degenerates. Reduced caudal ciliary array (arrow). **98.** Later exconjugant. Macronucleus (asterisks) reforms from numerous macronuclear anlagen (black arrowheads). Buccal apparatus (arrow); postgamic micronuclear division (white arrowhead). Ma, macronucleus. Scale bars 25 µm (95–98). **Fig. 99.** Phylogenetic tree inferred from SSrRNA gene sequences. Computed with PhyML based on the General Time-Reversible (GTR) model with gamma-distribution and estimate of invariable sites, as determined by Modeltest. Numbers at nodes represent bootstrap support of three different analyses: ML/NJ/MP (percent out of 500 and 1000 replicates, respectively). Asterisks indicate full support (100%) values for all three methods. /–/ indicates < 20% support for the respective method. Scale bar represents 10 changes per 100 positions. New species appears in bold face. **Fig. 100.** Phylogenetic tree inferred from partial COI gene sequences. Computed with PhyML based on General Time-Reversible (GTR) model with gamma-distribution and estimate of invariable sites, as determined by Modeltest. Numbers at nodes represent bootstrap support of three different analyses: ML/NJ/MP (percent out of 500 and 1000 replicates, respectively). Asterisks indicate full support (100%) values for all three methods. /–/ indicates < 20% support for the respective method. Nodes with < 20% support in all three methods are indicated by a single –. Scale bar represents 10 changes per 100 positions. New species appears in bold face.

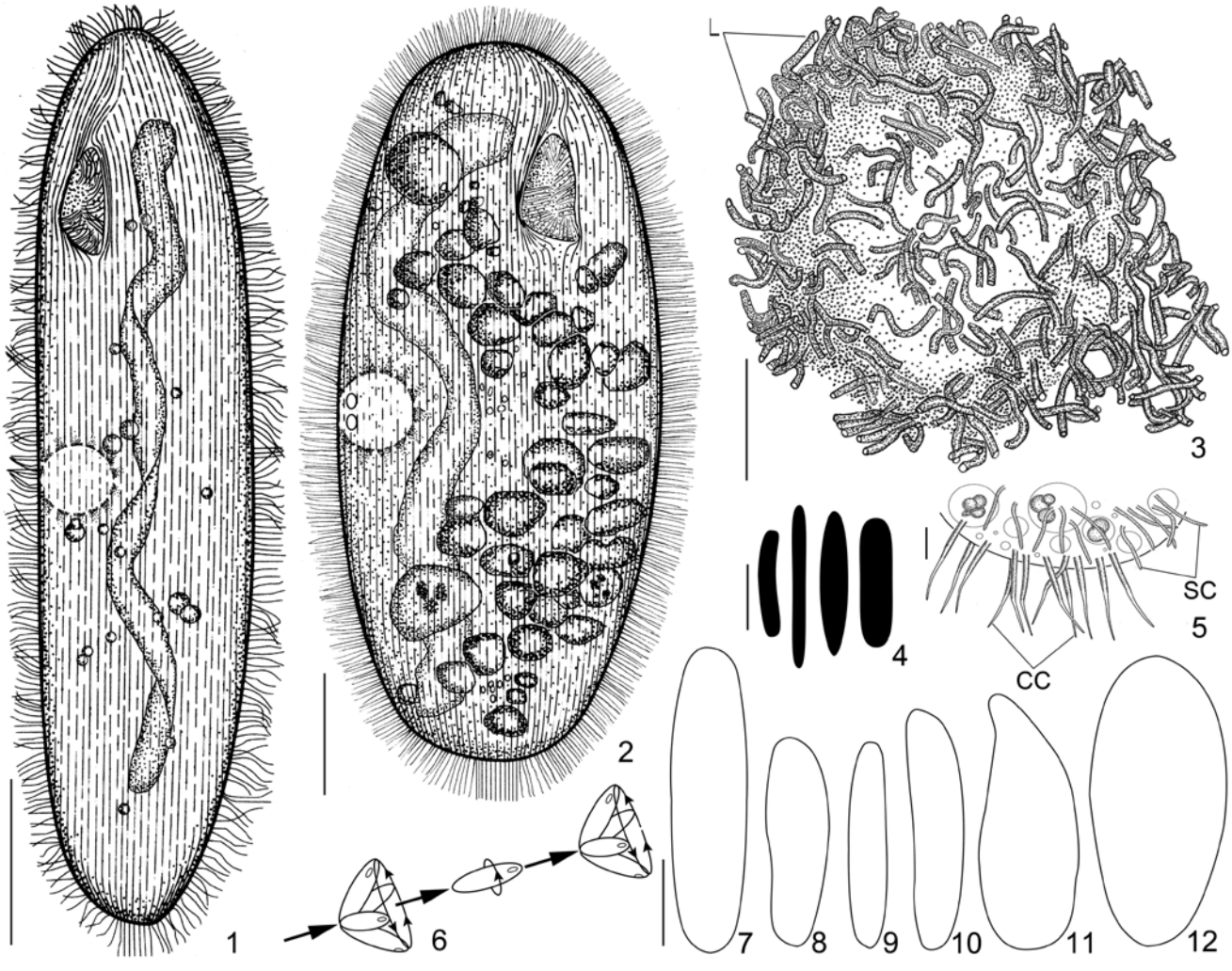

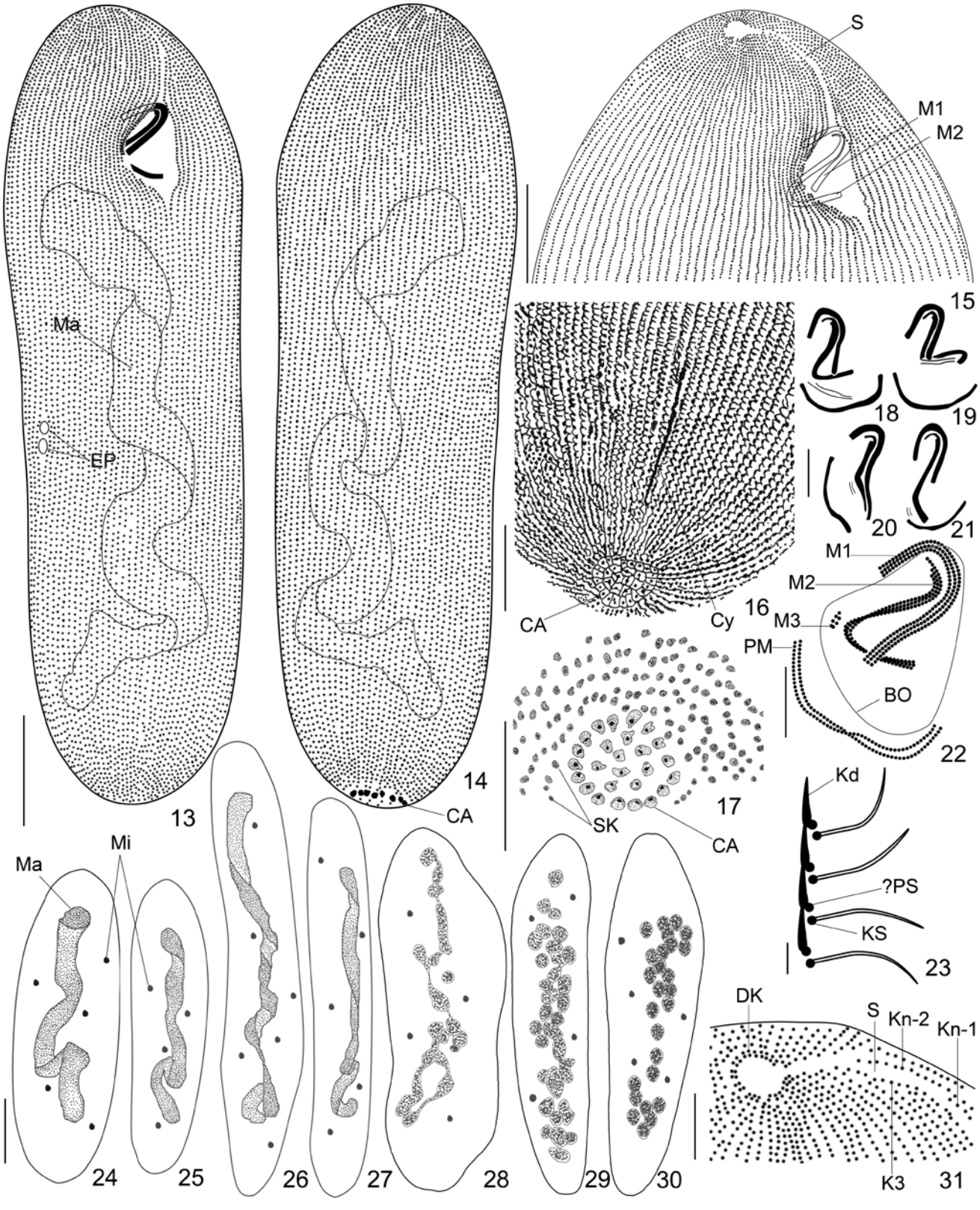

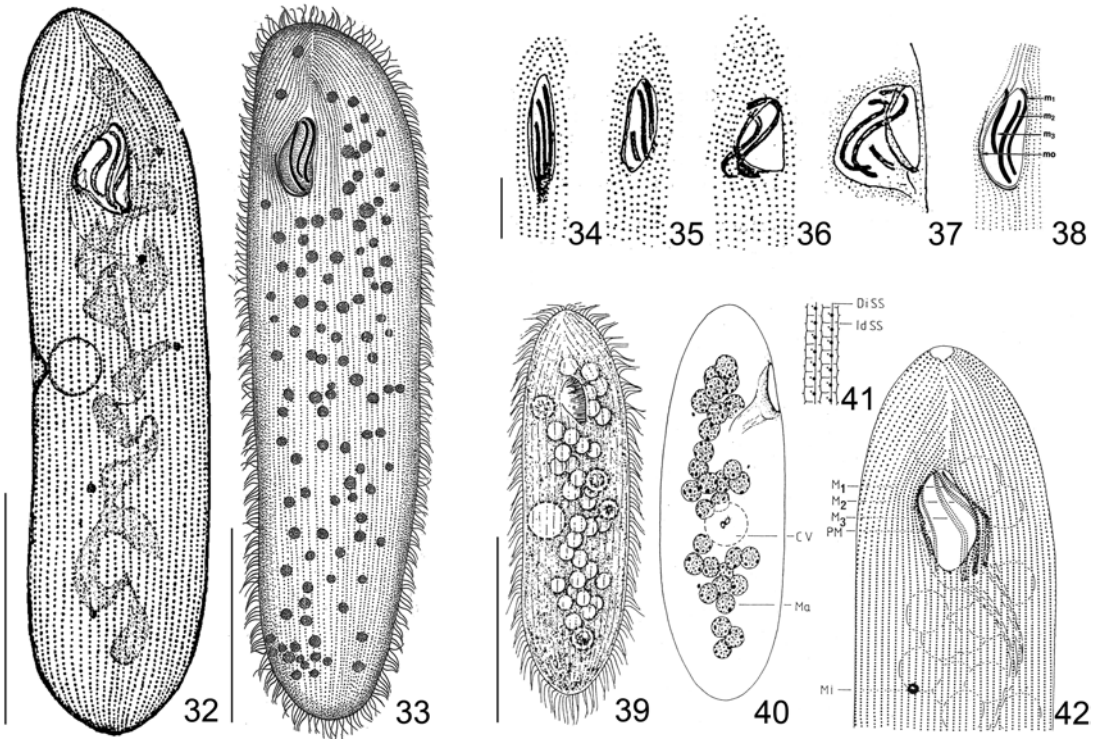

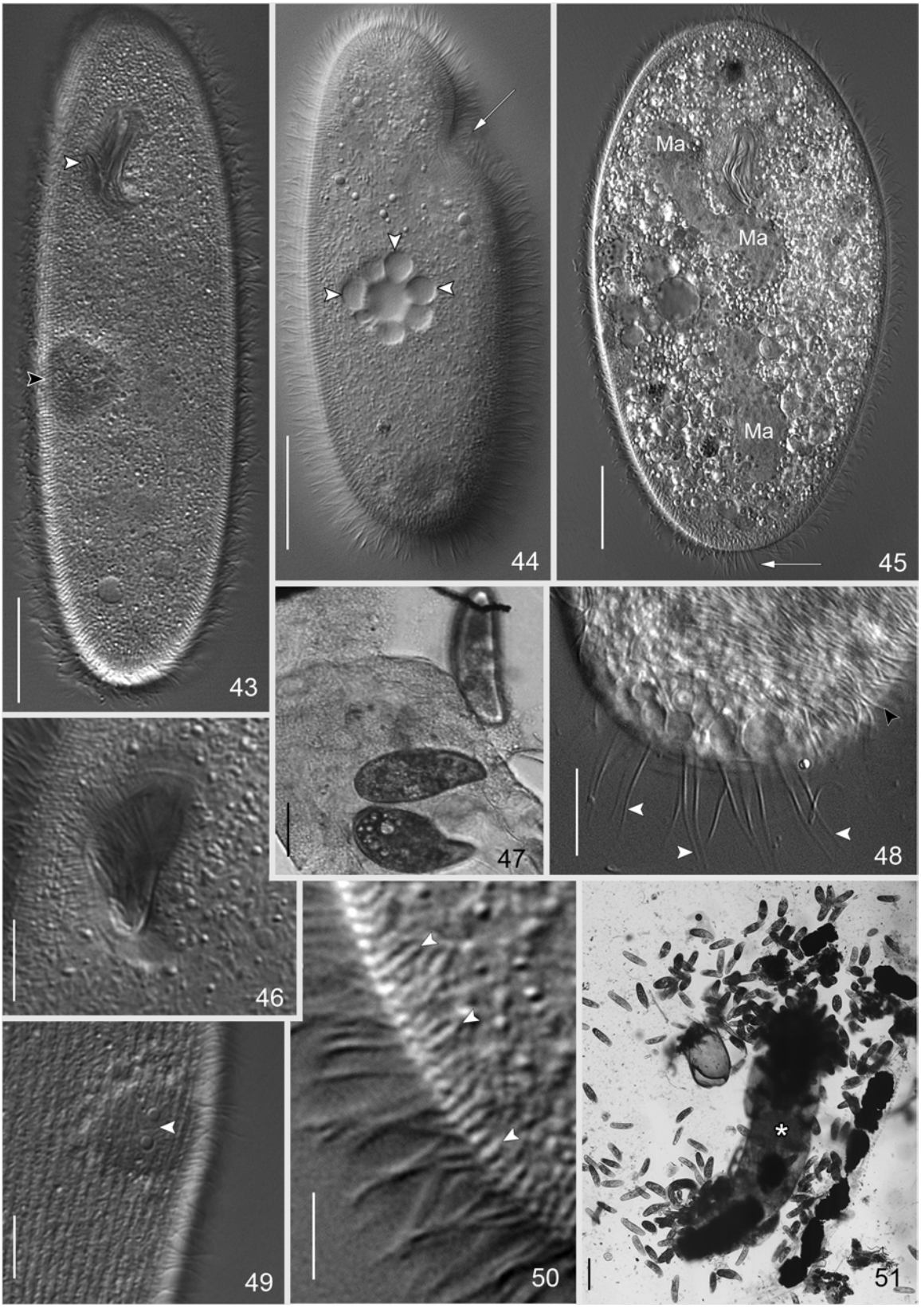

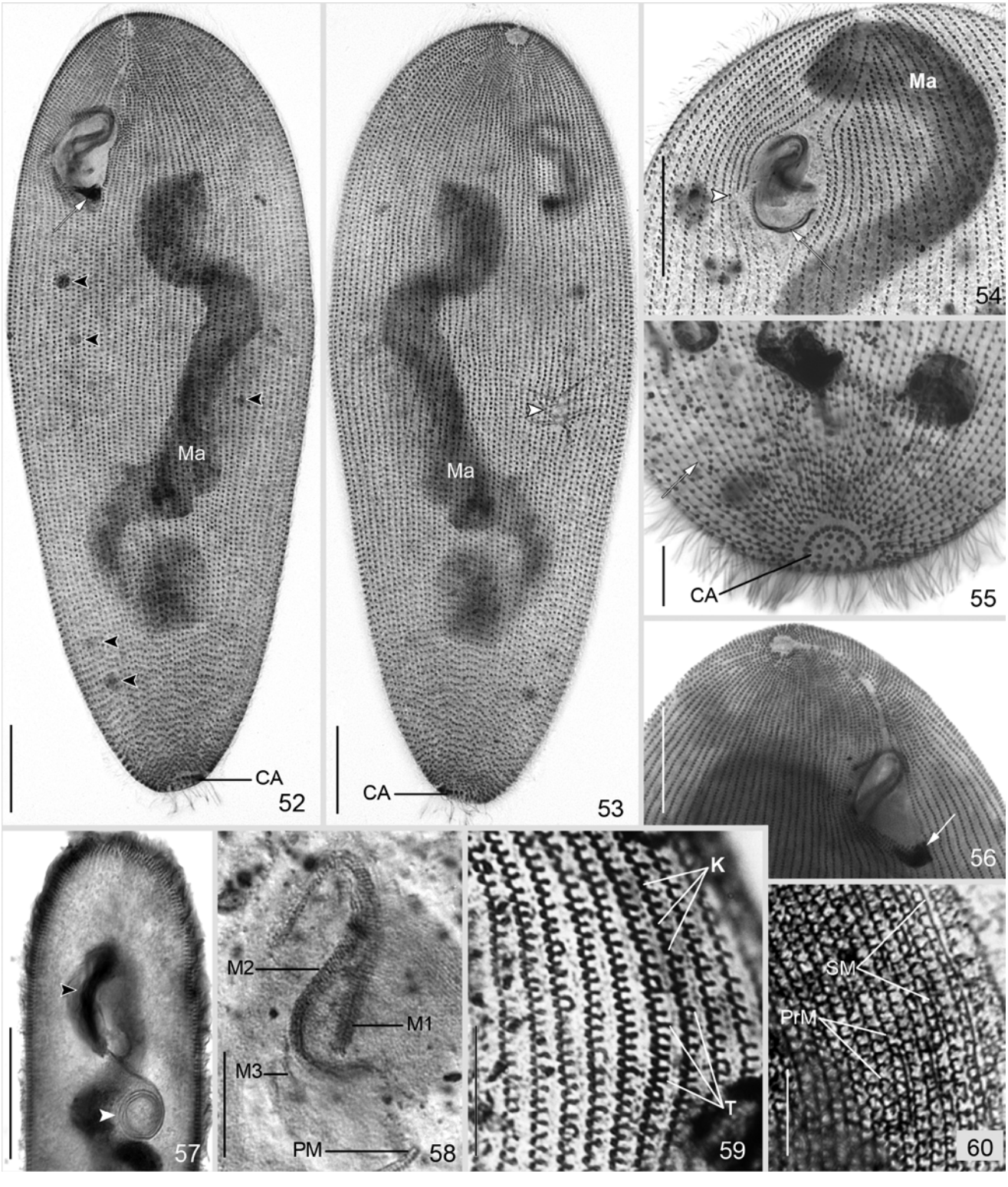

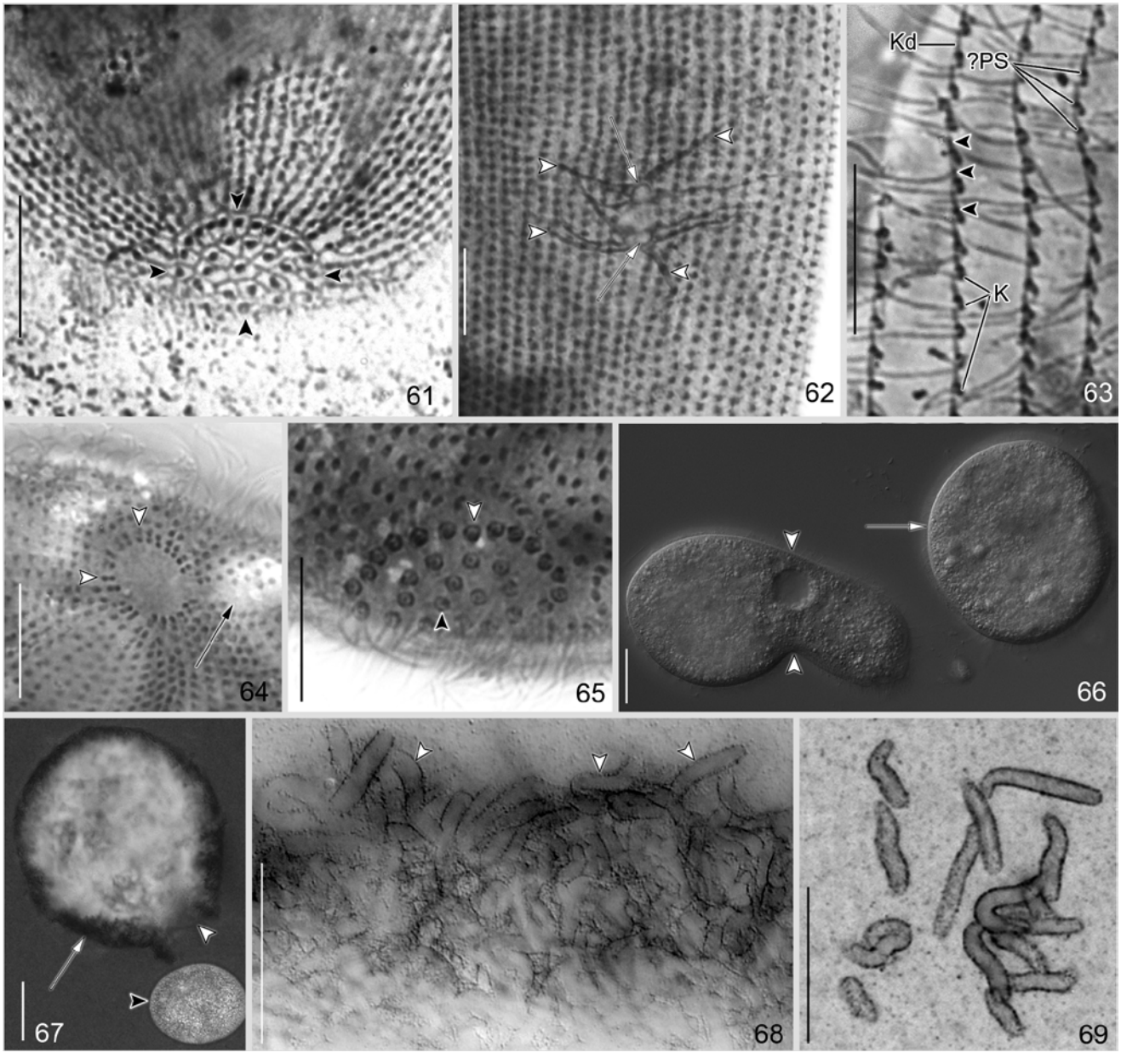

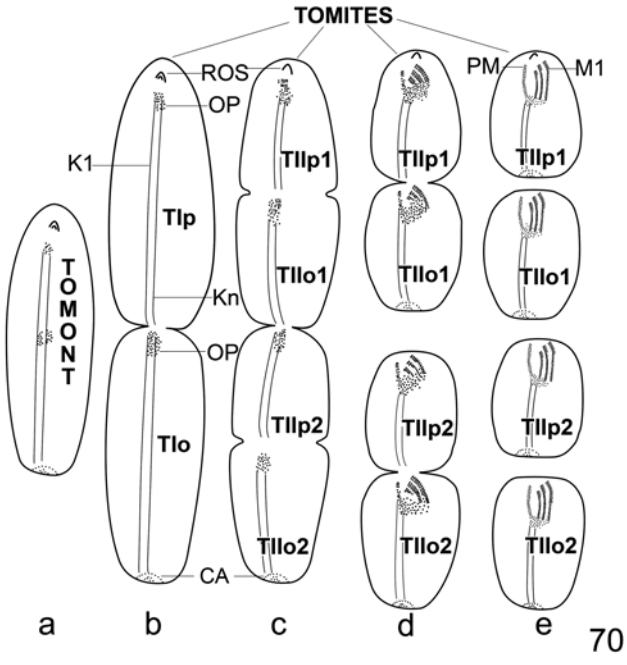

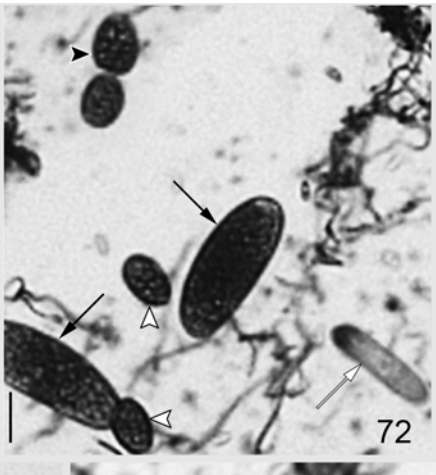

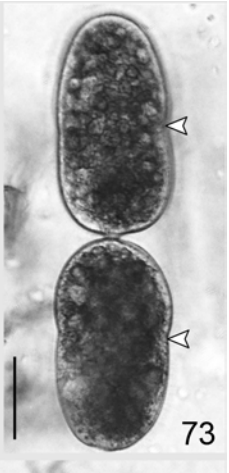

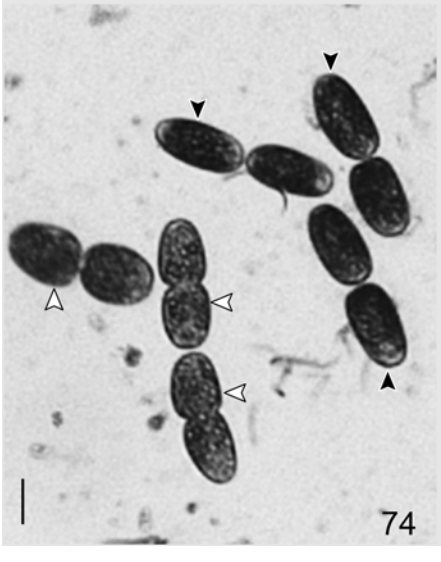

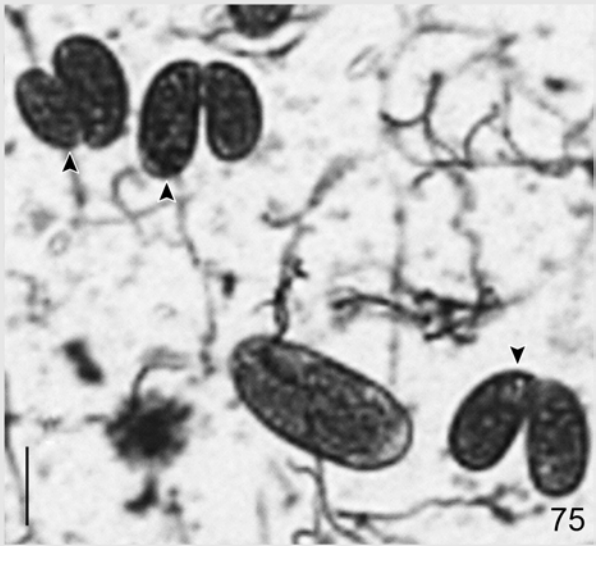

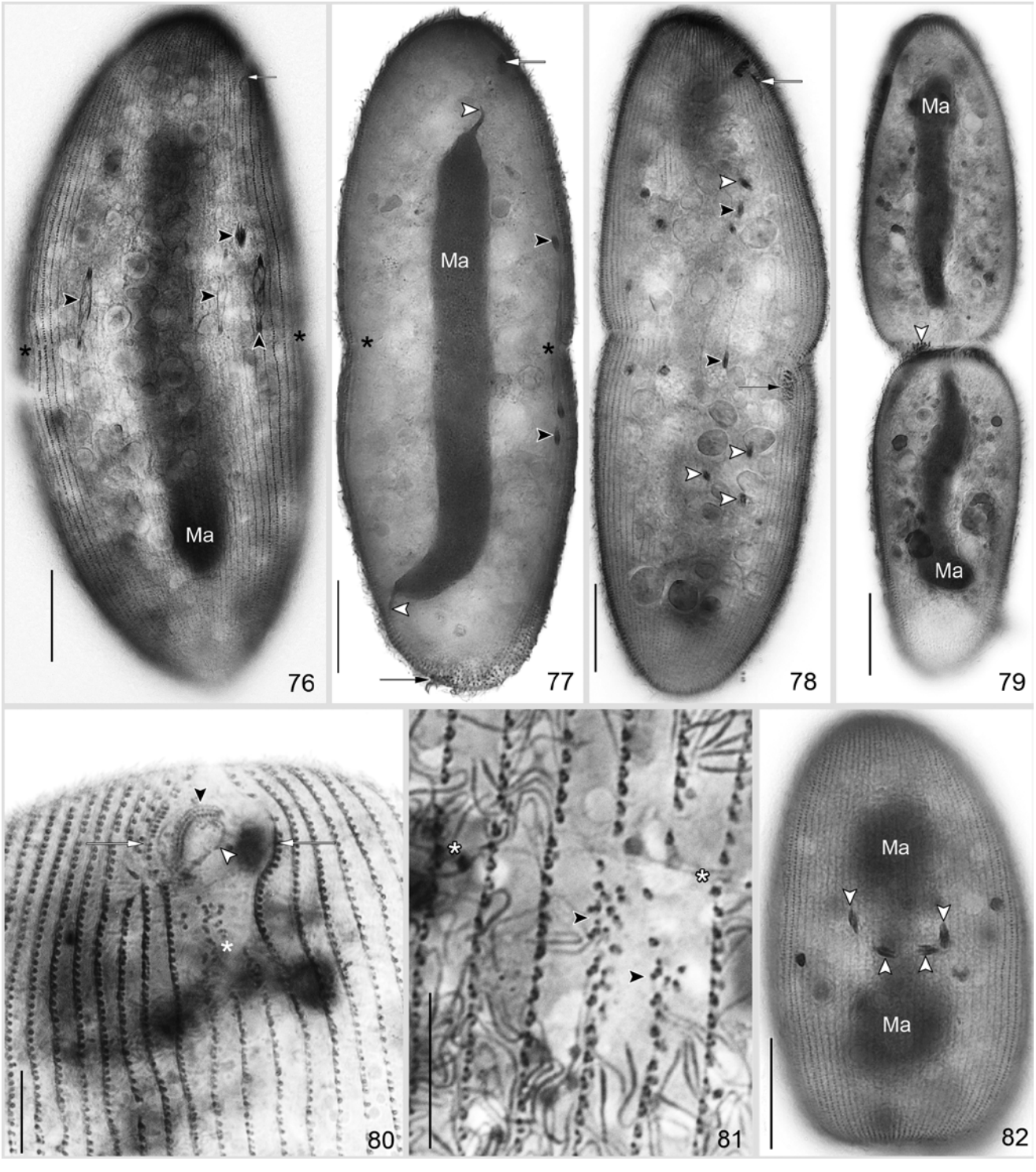

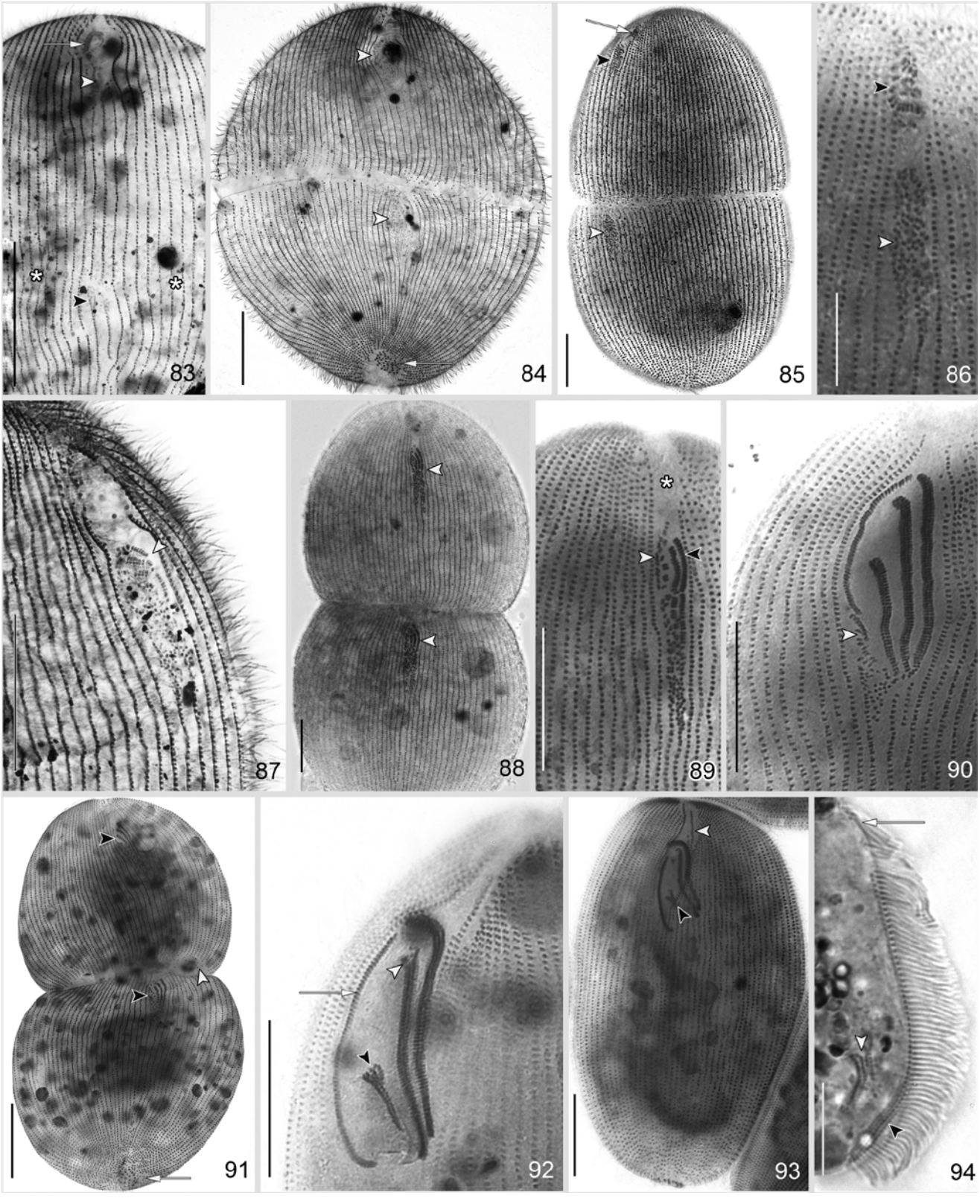

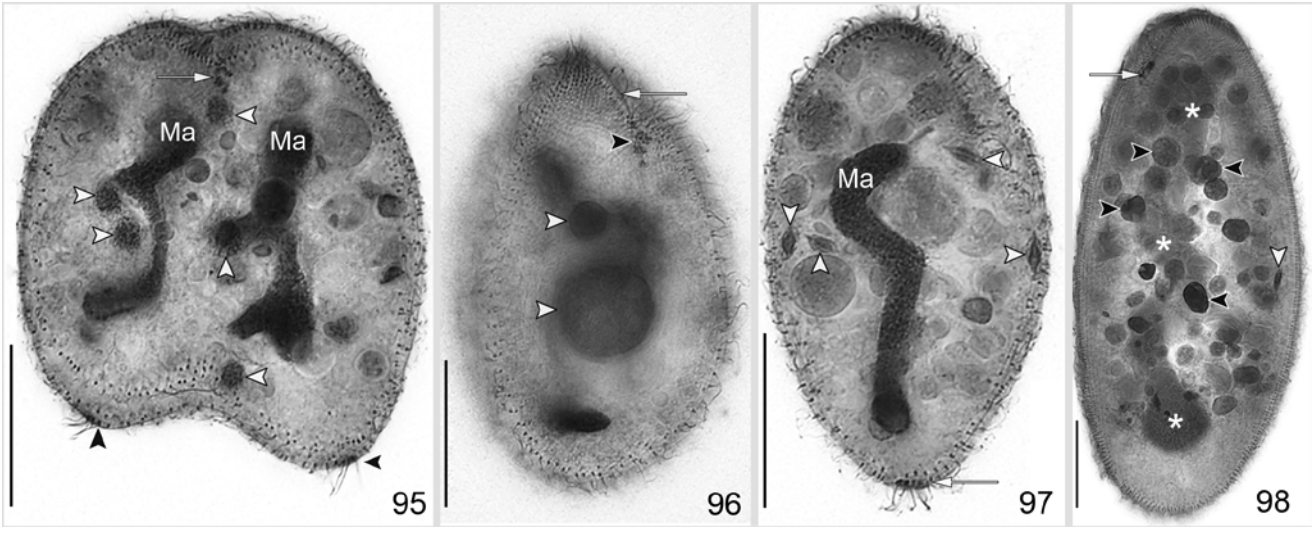

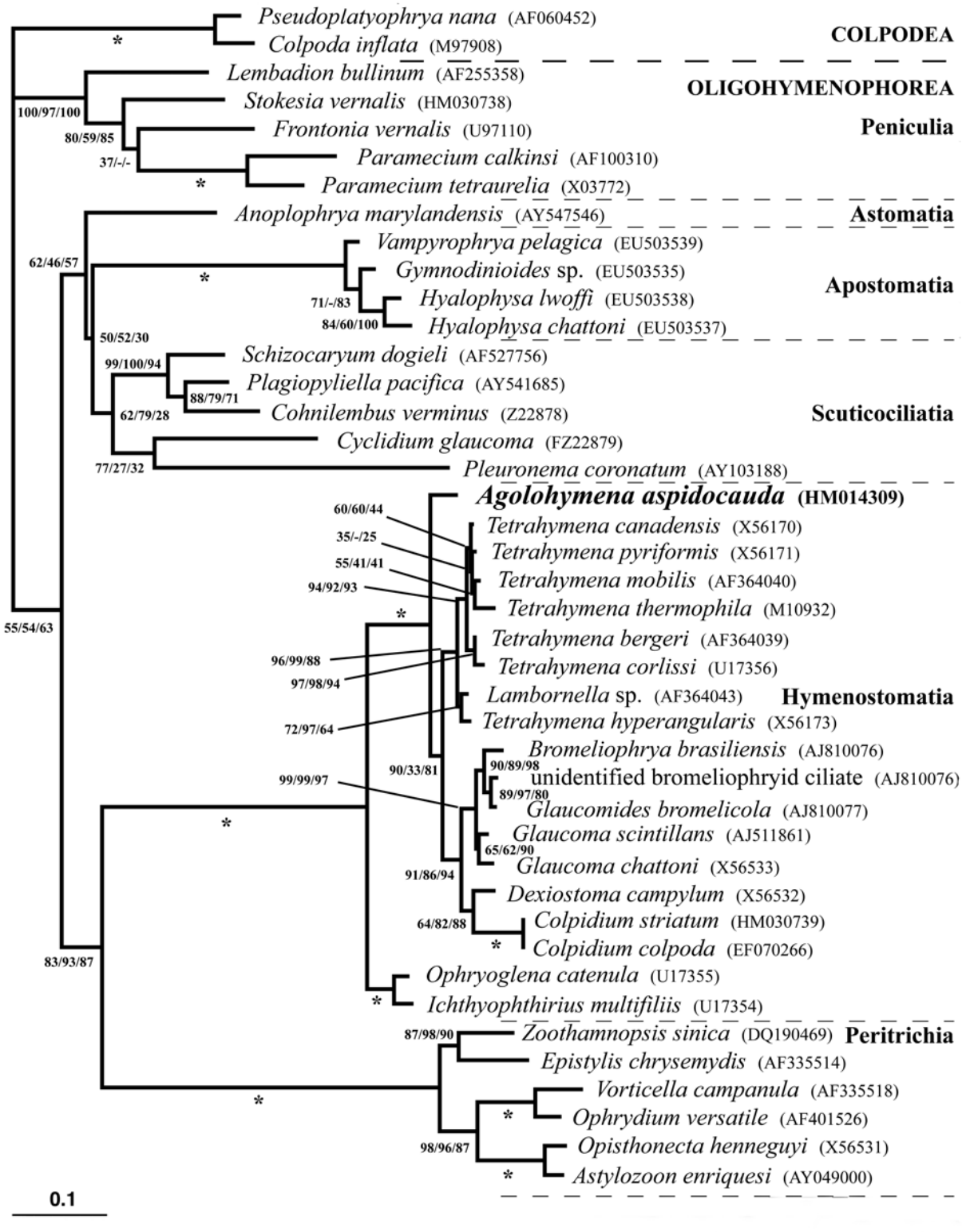

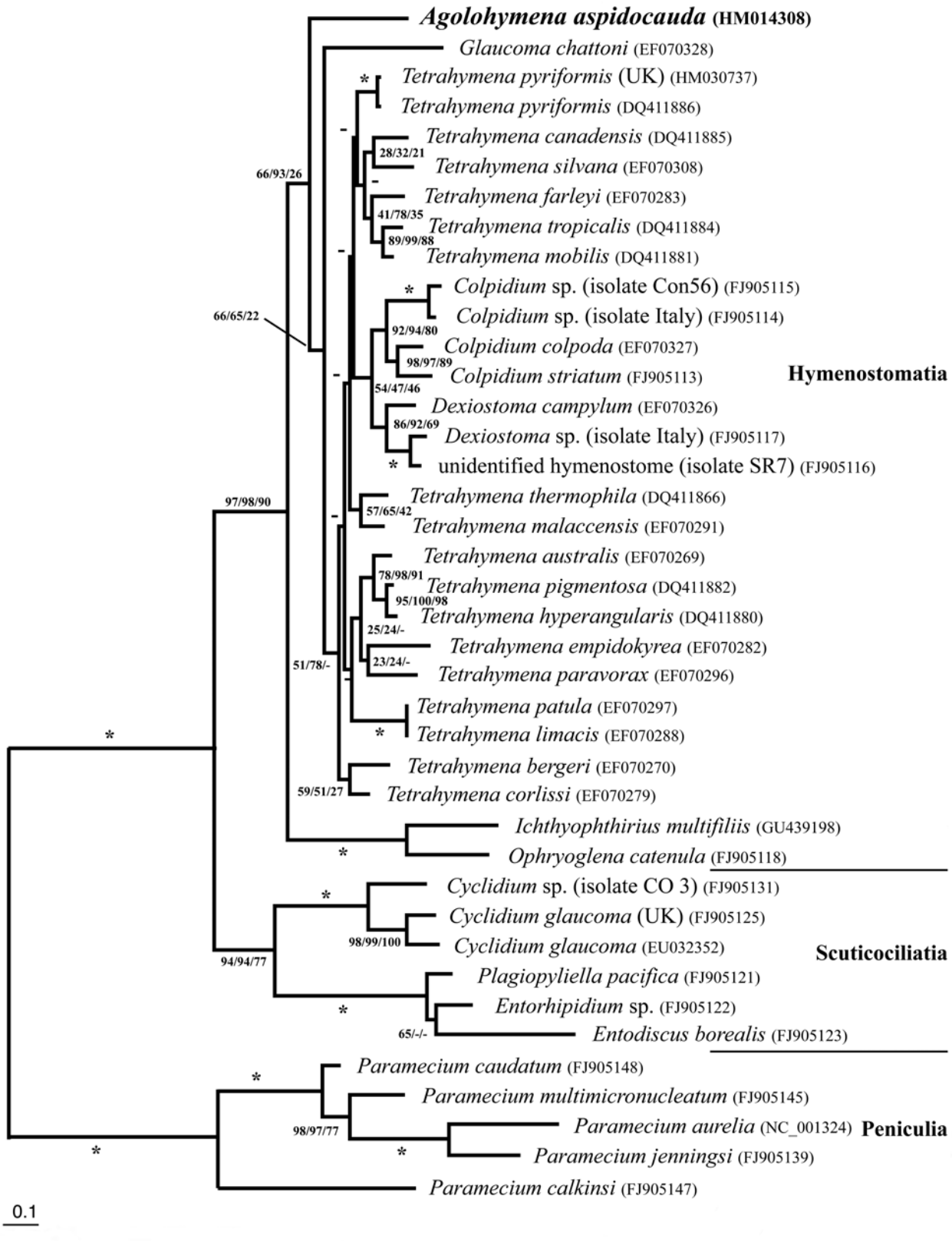

Table 1. Morphometric data on *Agolohymena aspidocauda* in vivo.

Characteristics[a]	Stage	$\bar{x}$	M	SD	CV	Min	Max	n
Body, length	Theront	150.3	150.0	15.96	10.6	114.0	185.0	58
	Trophont	154.8	154.0	19.95	12.9	97.0	202.0	100
	TI_p	109.3	107.0	15.16	13.9	91.0	153.0	16
	TI_o	106.0	103.0	13.01	12.3	85.0	132.0	16
	TII_{p1}/TII_{p2}[b]	55.3	55.0	7.56	13.7	45.0	67.0	13
	TII_{o1}/TII_{o2}[b]	51.0	52.0	6.86	13.4	40.0	66.0	13
	Conjugant 1[c]	70.0	71.0	7.20	10.3	55.0	82.0	31
	Conjugant 2	63.3	63.0	6.70	10.6	49.0	78.0	31
Body, width	Theront	38.8	39.0	5.19	13.4	29.0	52.0	58
	Trophont	62.8	61.0	10.46	16.6	37.0	97.0	100
	TI_p	59.2	59.0	6.01	10.1	48.0	74.0	16
	TI_o	60.1	61.0	6.73	11.2	48.0	78.0	16
	TII_{p1}/TII_{p2}	44.9	45.0	4.21	9.4	38.0	55.0	13
	TII_{o1}/TII_{o2}	43.5	43.0	3.97	9.1	37.0	54.0	13
	Conjugant 1	37.5	37.0	3.70	9.9	31.0	48.0	31
	Conjugant 2	35.6	37.0	3.92	11.0	27.0	41.0	31
Body, length:width ratio	Theront	3.9	3.9	0.46	11.8	2.9	4.9	58
	Trophont	2.5	2.5	0.30	12.1	1.7	3.3	100
	TI_p	1.9	1.9	0.22	11.8	1.5	2.1	16

TI_o	1.8	1.8	0.20	11.3	1.4	2.1	16
TII_{p1}/TII_{p2}	1.2	1.2	0.21	16.7	1.0	1.6	13
TII_{o1}/TII_{o2}	1.2	1.2	0.16	14.1	0.9	1.4	13
Conjugant 1	1.9	1.9	0.24	12.6	1.5	2.4	31
Conjugant 2	1.8	1.8	0.26	14.3	1.3	2.6	31

[a]Data from microphotographs of specimens in <3 week-old cultures. Trophonts were measured 6–8 hours after feeding; Tomites (TI_P, TI_o, $TII_{p1}/TII_{p2,}$, TII_{o1}/TII_{o2}) and conjugants were measured 18–22 hours after feeding. Measurements in µm.

CV, coefficient of variation (%); M, median; Max, maximum; Min, minimum; n, number of individuals investigated; SD, standard deviation; $\bar{x}$, arithmetic mean.

[b]See Figs 70a-e for definitions. TI_p, proter of the first division; TI_o, opisthe of the first division; TII_{p1}/TII_{p2}, pooled measurements of both proters of the second division; TII_{o1}/TII_{o2}, pooled measurements of both opisthes of the second division.

[c]Conjugant 1, larger conjugant of each anisogamic pair.

Table 2. Morphometric data on silver-impregnated specimens of *Agolohymena aspidocauda*.

Characteristics[a]	Method	$\bar{x}$	M	SD	CV	Min	Max	n
Body, length	P	131.8	131.0	22.38	17.0	83.0	178.0	100
Body, width	P	32.2	31.0	6.81	21.1	20.0	62.0	100
Body, length:width ratio	P	4.2	4.1	1.00	23.7	2.1	7.0	100
Anterior pole to distal end of M1, distance	P	22.9	22.0	5.42	23.7	16.0	39.0	25
Buccal overture, length	P	17.7	17.7	1.95	11.0	14.6	21.8	28

Buccal overture, width	P	6.8	6.8	1.03	15.2	4.6	10.0	28
Anterior end to excretory pores, distance[b]	P	71.1	71.0	10.12	14.2	50.0	98.0	33
Macronucleus, length	P	85.8	83.0	17.44	20.3	48.0	132.0	53
Macronucleus, width	P	8.1	7.9	1.59	19.7	5.6	12.0	53
Macronucleus, number	P	1.0	1.0	0.00	0.0	1.0	1.0	53
Micronucleus, diameter[c]	P	2.2	2.1	0.34	15.9	1.5	3.2	58
Micronucleus, number	P	6.1	6.0	0.79	12.9	5.0	7.0	20
Somatic kineties, number	P, PW, SC	88.4	90.0	5.65	6.4	74.0	96.0	29
Kinetids in a dorsal kinety, number	P, PW	164.5	155.0	28.58	17.4	122.0	210.0	11
Postoral kineties, number	P, PW, SC	2.2	2.0	0.53	23.6	1.0	4.0	43
Caudal ciliary array ring, diameter	P	9.5	9.0	2.59	27.2	5.6	15.0	38
Kinetids comprising ring of caudal ciliary array, number	P, PW, SC, SN	20.1	20.0	2.82	14.0	16.0	27.0	18
Kinetids enclosed by ring of caudal ciliary array, number	P, PW, SC, SN	12.1	12.0	3.08	25.5	7.0	20.0	18
Excretory pores, number	P	2.0	2.0	0.00	0.0	2.0	2.0	33

[a]Data based on permanent (P, SN) and temporary (PW, SC) mounts of theronts from 1–2 week-old cultures unfed for 24–36 hours. Measurements in µm. CV, coefficient of variation (%); M, median; Max, maximum; Min, minimum; M1, adoral membranelle 1; n, number of individuals investigated; P, protargol (protocol A, Bouin's-fixed); POM, paroral membrane; PW, protargol

(Wilbert protocol, Bouin's-fixed); SC, silver carbonate (formalin-fixed); SD, standard deviation; SN, dry silver nitrate protocol; $\bar{x}$, arithmetic mean.

[b]Distance from anterior end to anterior excretory pore.

[c]Measurements of 58 micronuclei in 10 individuals.